

# 島根大学学術情報リポジトリ **Shimane University Web Archives of kNowledge**

Title

Vertical changes in zooplankton abundance, biomass, and community structure at seven stations down to 3000 m in neighboring waters of Japan during the summer: Insights from ZooScan imaging analysis

Author(s)

Kunito Yamamae, Yasuhide Nakamura, Kohei Matsuno, Atsushi Yamaguchi

Journal

Progress in Oceanography, Volume 219, December 2023, 103155

Published

6 November 2023

URL (The Version of Record)

https://doi.org/10.1016/j.pocean.2023.103155

この論文は出版社版でありません。 引用の際には出版社版をご確認のうえご利用ください。

This version of the article has been accepted for publication, but is not the Version of Record.

Vertical changes in zooplankton abundance, biovolume, and community structures at seven stations down to the greater depths (~3000 m) covering neighboring waters around Japan during the summer: Insights from the imaging analyses (ZooScan)

Kunito Yamamae<sup>a,1</sup>, Yasuhide Nakamura<sup>b</sup>, Kohei Matsuno<sup>a,c</sup>, and Atsushi Yamaguchi<sup>a,c,\*</sup>

\*\*Faculty/Graduate School of Fisheries Sciences, Hokkaido University, 3-1-1 Minato-cho, Hakodate, Hokkaido 041–8611, Japan

\*\*Estuary Research Center, Shimane University, 1060, Nishikawatsu-cho, Matsue 690–8504, Japan

\*\*Arctic Research Center, Hokkaido University, Kita-21 Nishi-11 Kita-ku, Sapporo, Hokkaido, 001–0021, Japan

\*\*Present address: Ishikawa Prefecture Fisheries Research Center, 1-1 Kuratsuki, Kanazawa, Ishikawa, 920–858, Japan

\*\*corresponding author, E-mail: a-yama@fish.hokudai.ac.jp

Keywords: Size spectrum, NBSS, Inter-oceanic comparison, ZooScan, Size diversity

# **Abstract**

 $1^{15}$ 

<sup>2</sup>16

 $^{11}_{12}$ 21

14

1**7**24

2830

30<sup>3</sup>1

31<sub>32</sub>32

The imaging device ZooScan is used for the net-collected zooplankton samples. The application of ZooScan is made mostly for the regional or seasonal changes in the zooplankton community, and a scarce attempt was made for vertical changes, especially down to the deep sea. In this study, we made ZooScan analysis on zooplankton samples collected by vertically stratified zooplankton samples collected by VMPS down to 3000 m at seven stations of the various neighboring waters of Japan covering: the Okhotsk Sea, Japan Sea, East China Sea, and subarctic, transitional, and subtropical North Pacific. Throughout the region, both abundance and biovolume decreased with increasing depths. ANCOVA analysis revealed that the affecting factors on the vertical changes varied with the unit. Thus, depth and region were the prime important factors for determining abundance and biovolume, respectively. Cluster analysis based on abundance separated the zooplankton community into 8 groups. The occurrence of each group varied regionally and 3-5 groups occurred vertically stratified for each station. Common for all the stations, Normalized Biomass Size Spectra (NBSS) and size diversity showed great vertical changes around 150-500 m depths. For the shallower depths, the NBSS slope was steep, the intercept was high, and size diversity was low. For the deeper depths, opposite changes were the cases of each parameter. The generalized additive models revealed that various environmental parameters (depth, temperature, and salinity) had a significant effect on NBSS and size diversity. This study indicates that the imaging method may be useful even for the analysis of the deep-sea zooplankton community.

1. Introduction

5966 $^{60}_{61}\!\!67$ 

62

63 64 65

In marine ecosystems, zooplankton feed on primary production by phytoplankton, change the organic material sizes into large, and have a role in mediating or transferring the organic materials to the higher trophic levels (cf. Lalli and Parsons, 1997; Miller and Wheeler, 2012). On the other hand, zooplankton egests fecal pellets and performs diel vertical migration, which has a function to accelerate vertical material fluxes termed "Biological pump" (Ducklow et al., 2001; Steinberg et al., 2008a). Based on the zooplankton taxa, their feeding modes and foods are greatly varied with taxa (cf. Lalli and Parsons, 1997; Miller and Wheeler, 2012). On the other hand, zooplankton sizes determine the sizes of the predation available sizes of the vertebrate predators (Nunn et al., 2012). Zooplankton sizes also affect the fecal pellet sizes, which are directly related to the sinking rates of the fecal pellets (Stamieszkin et al., 2015). Thus, zooplankton size and taxa are the two most important factors in determining their quantitative functional roles in marine ecosystems.

As the device to obtain size and taxonomic information on zooplankton simultaneously, the imaging device: ZooScan is available (Gorsky et al., 2010; Irisson et al., 2022). From ZooScan data, as indices of zooplankton size spectra, analyses on Normalized Biomass Size Spectra (NBSS) are also possible (Schultes and Lopes, 2009; Kwong and Pakhomov, 2021). Both the slope and intercept of NBSS are known to be varied with the affection of the bottom-up or top-down controls. Thus, high primary production induced by the high nutrient providing, which induces a high abundance of the small-sized zooplankton (e.g. bottom-up conditions), intercept and slope of NBSS is high and steep, respectively, while the under the high predation pressure conditions on the smalls-zed zooplankton (top-down condition), the intercept and slope of NBSS change to low and flat, respectively (Moore and Suthers, 2006; Suthers et al., 2006; Zhou, 2006; Zhou et al., 2009). As the studies on NBSS based on ZooScan data, most studies conducting on seasonal changes on one occasion (Vandromme et al., 2012) and spatial changes for the epipelagic depths (Naito et al., 2019; Kwong and Pakhomov, 2021). Few attempts and applications were made on the vertical changes in the zooplankton size community by using ZooScan.

The neighboring waters of Japan include subarctic, transitional, and subtropical regions of the western North Pacific and three marginal seas: Okhotsk Sea, Japan Sea, and East China Sea, all of them having different oceanographic characteristics. As the studies treated zooplankton size composition in the neighboring waters of Japan, latitudinal changes along the north-south transect (Yokoi et al., 2008; Shiota et al., 2013; Mishima et al., 2019), inter-oceanic comparison including marginal seas (Sato et al., 2015), and seasonal changes at one location (Yamaguchi et al., 2014; Hikichi et al., 2018) are available. While these studies are valuable, all data of these studies were collected by the Optical Plankton Counter (OPC; Herman, 1988). Because of the device (OPC), there included no taxonomic data. It also should be noted that they studied mainly the epipelagic depths.

31<sub>86</sub> 32<sup>86</sup> 33<sub>87</sub> 

35<u>88</u> 

 No attempt was made on the vertical changes in zooplankton size composition, especially down to the greater depths.

As the studies conducted vertical changes in zooplankton community down to the greater depths in the neighboring waters of Japan, studies on latitudinal changes in zooplankton biomass in the subarctic, transitional, and subtropical regions of western North Pacific (Yamaguchi et al., 2002b, 2004, 2005), species-specific distributions of copepods (Yamaguchi et al., 2002a), and chaetognaths (Ozawa et al., 2007) are available. While these studies are important, since they are not targeting whole zooplankton communities, vertical, inter-oceanic changes in zooplankton size and taxonomic compositions remain unclear around the neighboring waters of Japan.

In this study, we conducted ZooScan analyses on the vertically stratified zooplankton samples down to a maximum of 3000 m collected at seven stations covering subarctic, transitional, and subtropical regions of the western North Pacific, and three marginal seas: Okhotsk Sea, Japan Sea, and the East China Sea. Zooplankton abundance, biovolume, community structure, size composition, and NBSS were evaluated and their geographical and vertical changing patterns were evaluated. For abundance and biovolume, their vertical changing patterns were evaluated by analyzing the regressions with depth and comparing their regressions with those from the previous studies. Based on the abundance of each taxon, zooplankton community structures were analyzed by cluster analyses, and their spatial and vertical distributions were conducted. As indices of zooplankton size compositions, intercept and slope of NBSS, and size diversity were analyzed for each sample, and the effects of the environmental parameters (depth, temperature, and salinity) on them were analyzed by the Generalized Additive Models (GAM).

## 2. Material and methods

# 2.1. Field sampling

Vertically stratified zooplankton samplings were conducted at seven stations in the western North Pacific and marginal seas around Japan through cruises of T/S *Oshoro-Maru* from 11 June to 2 August 2011 and 10–15 June 2014. For station codes and sampling depths are follow: St. OK in the southern Okhotsk Sea (45°24′N, 145°02′E) from 0–3000 m, St. JS1 (41°45′N, 138°30′E) and JS2 (41°45′N, 139°47′E) in the Japan Sea both from 0–750 m, St. ECS (27°18′N, 126°48′E) in the East China Sea from 0–1500 m, St. SA (43°39′N, 154°07′E) in the subarctic western North Pacific from 0–3000 m, St. TR (36°30′N, 155°00′E) in the transitional domain of the western North Pacific from 0–3000 m, and St. ST (20°47′N, 135°29′E) in the subtropical western North Pacific from 0–1000 m. Samplings were conducted by Vertical Multiple Plankton Sampler (VMPS) equipped with 63 μm mesh with 0.25m² mouth opening (Tsurumi Seiki Co. Ltd., Terazaki and Tomatsu, 1997) with twelve maximum stratifications (Fig. 1, Table 1). Zooplankton samples were preserved with 5% borax-

51934 60 61<sub>1</sub>35

62

63 64 65 buffered formalin seawater on board immediately after collection. Hydrographic data (temperature, salinity, and dissolved oxygen [DO]) were obtained by CTD (SBE 911 Plus, Sea–Bird Electronics Inc.) casts at each station.

# 2.2. ZooScan measurement

In the land laboratory, zooplankton by images were captured ZooScan (Hydrooptic Inc.) based on the protocol of Gorsky et al. (2010). Firstly the background scan was conducted by filling distilled water in the cell. Then the zooplankton samples with whole to the subsamples at 1/15 maximum dividing rates made by the widebore pipet were placed on the ZooScan scanning cell and scanned. The obtained images were separated with each individual by using ZooProcess with the aid of ImageJ software. The images were digitalized with a resolution of 2400 dpi which corresponded to 10.6 µm for one pixel. Each image was uploaded to the website EcoTaxa, and semiauto identification was made for each image (Picheral et al., 2017; Irisson et al., 2022).

Identification of taxa was made with the following categories: protozoan; Phaeodaria, Foraminifera, Tintinnida, and metazoan; Cnidaria, Hydrozoa, Scyphozoa, Siphonophorae, Annelida, Gymnosomata, Ostracoda, Calanoida, Cyclopoida, Harpacticoida, Poecilostomatoida, Mysidacea, Amphipoda, Euphausiacea,

Sampling data on vertical stratified samplings by VMPS equipped 63 µm mesh at the seven stations located various regions of the neighboring waters of Japan. Note that the depth strata was varied with the region

	Depth strata (m)	0–25, 25–50, 50–75, 75–100, 100–150, 150–250, 250–500, 500–750, 750–1000, 1000–1500, 1500–2000, 2000–3000	0-50, 50-150, 150-250, 250-550, 550-600, 600-750	0-50, 50-150, 150-250, 250-400, 400-600, 600-750	0–25, 25–50, 50–75, 75–100, 100–150, 150–250, 250–375, 375–500, 500–750, 750–1000, 1000–1250, 1250–1500	0–25, 25–50, 50–75, 75–100, 100–150, 150–250, 250–500, 500–750, 750–1000, 1000–1500, 1500–2000, 2000–3000	0–25, 25–50, 50–75, 75–100, 100–150, 150–250, 250–500, 500–750, 750–1000, 1000–1500, 1500–2000, 2000–3000	0–25, 25–50, 50–75, 75–100, 100–150, 150–250, 250–500, 500–750, 750–1000
Ţ	D/N	Night	Night	Night	Day	Night	Day	Night
	Sampling data D/N	11 June 2011	11 June 2014	14 June 2014	4 July 2011	31 July 2011	27 July 2011	11 July 2011
•	Position	45°24′N, 145°02′E	41°45′N, 138°30′E	41°45N, 139°47E	27°18′N, 126°48′E	43°39′N, 154°07′E	36°30′N,155°00′E	20°47′N,135°29′E
	Abbreviation	OK	JS1	JS2	ECS	SA	TR	ST
	Area	Okhotsk Sea	Japan Sea (Station 1)	Japan Sea (Station 2)	East China Sea	NW Pacific: subarctic region	NW Pacific: transitional region	NW Pacific: subtropical region
nc	licu	laria,	Opł	niur	oidea,	Moll	usca,	Decap

Calyptopis, Cladcera, Chaetognatha, Doliolida, Appendicularia, Ophiuroidea, Mollusca, Decapoda,

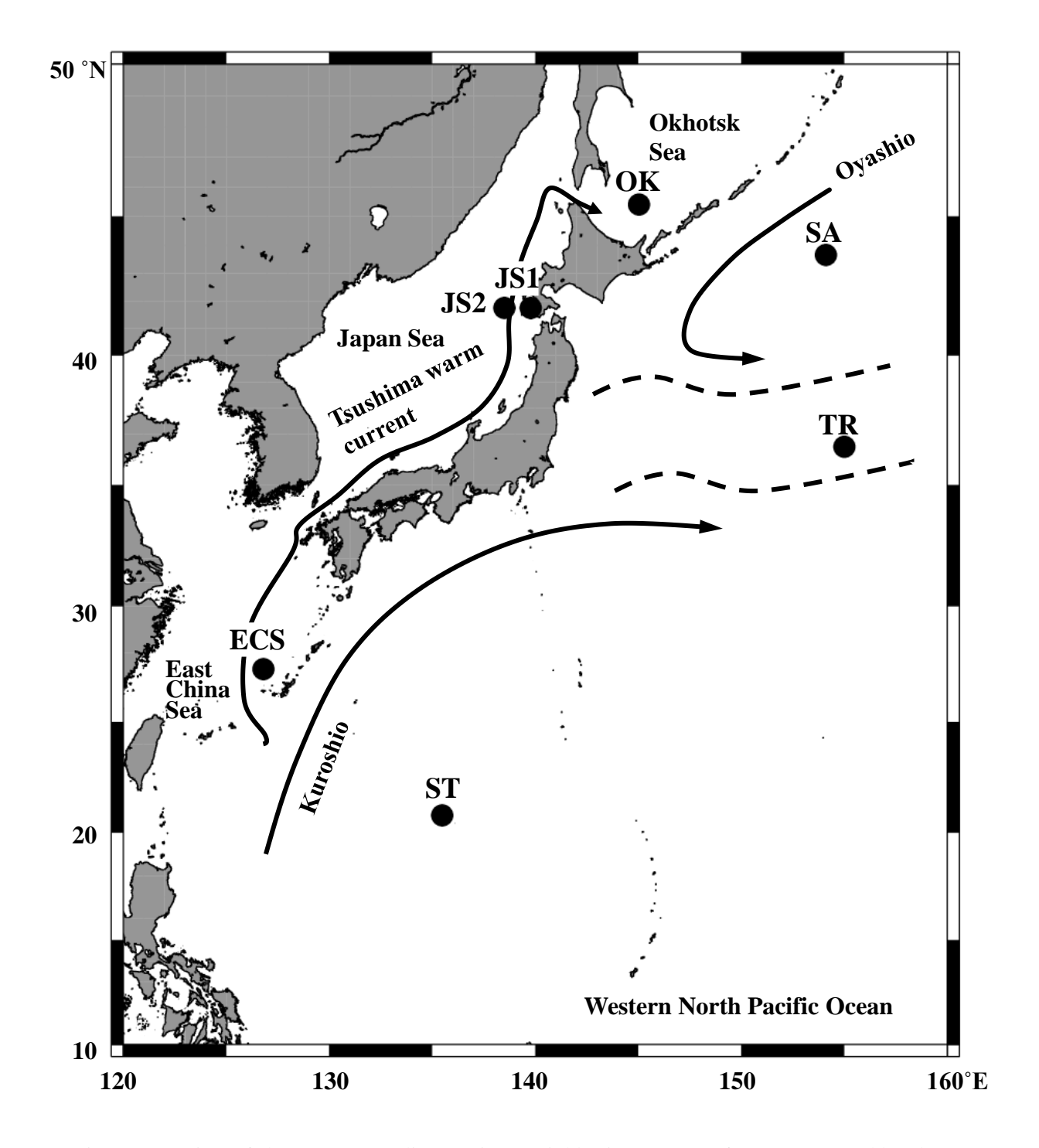


Fig. 1. Location of the seven sampling stations neighboring waters of Japan. OK: Okhotsk Sea, JS1: Japan Sea station 1, JS2: Japan Sea station 2, ECS: East China Sea, SA: subarctic Pacific, TR: transitional Pacific, ST: subtropical Pacific. Approximate flow directions of the major currents are shown with the arrows in the panel.

Crustacean nauplius, and others; fecal pellet, fragment, detritus. For the numerical dominant Calanoida, more detailed identifications were possible for the following genera: *Acartia* spp., *Eucalanus bungii, Gaetanus* spp., *Metridia* spp., *Neocalanus* spp., *Paraeuchaeta* spp., *Pseudocalanus* spp. Within the above categories, non-living fractions: fecal pellet, fragment, and detritus were excepted from the following analyses.

Based on the ZooScan images, the volume (Volume, mm<sup>3</sup>) of each specimen was calculated

5<u>1</u>872 

 ${6\!\!10}{73}$ 

 from the major axis length ( $L_{major}$ , mm) and the minor axis length ( $L_{minor}$ , mm) by using the following equation:

*Volume* = 
$$4/3 \times \pi \times (L_{major}/2) \times (L_{minor}/2)^2$$

For the size of each specimen, the equivalent spherical diameter (ESD, mm) was calculated from the biovolume using the following equation:

$$ESD = \sqrt[3]{\frac{Volume \times 3}{4\pi}}$$

Based on the numbers (n), the volume of the specimen  $(Volume, mm^3)$ , net filtering volume  $(F: m^{-3})$ , abundance  $(Abu: ind. m^{-3})$ , and biovolume  $(Bio: mm^3 m^{-3})$  were quantified from the following equations:

$$Abu = \frac{n}{F \times s}$$

$$Bio = \frac{Volume}{F \times s}$$

where s is the splitting factor of the samples during the ZooScan measurements.

# 2.3. Data analysis

While we applied smaller mesh sizes (63  $\mu$ m) for the collection of the zooplankton to avoid the effects of collection efficiency of the smaller specimens, which may be varied with the samples due to the abundance of the seston or detritus (cf. Makabe et al., 2012), we quantified zooplankton for larger than 0.20 mm ESD in this study. Which is fairly larger than the diagonal length of the applied mesh (0.089 mm).

To evaluate vertical changes in abundance and biovolume, regression analysis applying dependent variables as abundance (*Abu*: ind. m<sup>-3</sup>) or biovolume (*Bio*: mm<sup>3</sup> m<sup>-3</sup>) and independent variable as depth (*D*: m). For the regressions, we applied log-log transformed values for each variable and analyzed by the solver function of the MS-Excel:

$$\log_{10} Abu = a \times \log_{10} D + b$$
$$\log_{10} Bio = a \times \log_{10} D + b$$

where a is the slope and b is the intercept of the regression. To evaluate the effects of depths and regions (area), we made an analysis of covariance (ANCOVA) by applying target variables such as abundance and biovolume and explanation variables such as depth and area.

To evaluate the zooplankton community of each sample, based on the values transferred to the fourth root of the abundance (*Abu*: ind. m<sup>-3</sup>), we classified and made cluster analyses for the zooplankton community of the total 69 samples by the Bray-Curtis similarities connecting the mean-connecting methods. Inter-group differences in zooplankton abundance were analyzed by one-way

 ANOVA and post hoc test (Tukey-Kramer test). For the effects of the environmental variables (latitude, depth, temperature, salinity, and dissolved oxygen), we made multiple linear regression analyses for the two-dimensional non-metric multidimensional scaling (NMDS) of the result of the Bray-Curtis analysis.

As data source of the normalized biomass size spectra (NBSS), we applied zooplankton biovolume data at 0.2-5.0 mm ESD quantified with 0.05 mm intervals NBSS. For NBSS, as the *X*-axis, we applied  $\log_{10}$  zooplankton biovolume (mm³), the value of the biovolume of each size class (mm³) converted into a common logarithm. For the *Y*-axis of the NBSS, we applied  $\log_{10}$  zooplankton biovolume (mm³ m³) /  $\Delta$ biovolume (mm³). The biovolume was divided by the biovolume interval ( $\Delta$ biovolume [mm³]) and converted to a common logarithm. Based on these data, the NBSS linear model was calculated as follows:

$$Y = aX + b$$

where a and b are the slope and intercept of the NBSS, respectively.

Zooplankton size diversity was calculated by the methods of species diversity (H') (Morishita, 1996). For evaluation of the effects of the environmental variables (depth, temperature, and salinity) on the slope, the intercept of the NBSS, and size diversity, analyzed by the generalized additive model (GAM), were made for each target variable. We applied R for such statistical analyzes.

#### 3. Results

### 3.1. Hydrography

Vertical changes in temperature, salinity, and DO at each station are shown in Fig. 2. Throughout the station, temperatures ranged from -1.2 to  $29.4^{\circ}$ C. Inter-oceanic differences in temperature were prominent for the upper 1500 m. The warmest conditions were in the cases of the subtropical Pacific and the East China Sea, while the coldest condition was observed for the Okhotsk Sea. Temperature below  $0^{\circ}$ C was seen for 50-100 m depths of the Okhotsk Sea. Such "intermediate cold water" (Takizawa, 1982) was also seen in the subarctic Pacific. The other special water mass, "Japan Sea proper water," which is characterized by the extremely cold temperature ( $0-1^{\circ}$ C) (Sudo, 1986), was seen below 300 m depths of the Japan Sea.

Salinity ranged between 32.6 and 34.9 throughout the stations. The regional changes were prominent for the above 1500 m depths and classified into three patterns: subarctic, subtropical, and Japan Sea. For the subarctic (St. OK, SA), salinity was low at the near-surface layer and then increased with increasing depth. For the subtropical (St. ECS, TR, ST), the high salinity near the surface formed a subsurface minimum of around 200–700 m, then increased with increasing depths below that layer. For the Japan Sea (St. JS1, JS2), salinity was at a narrow range (34.0–34.3) and

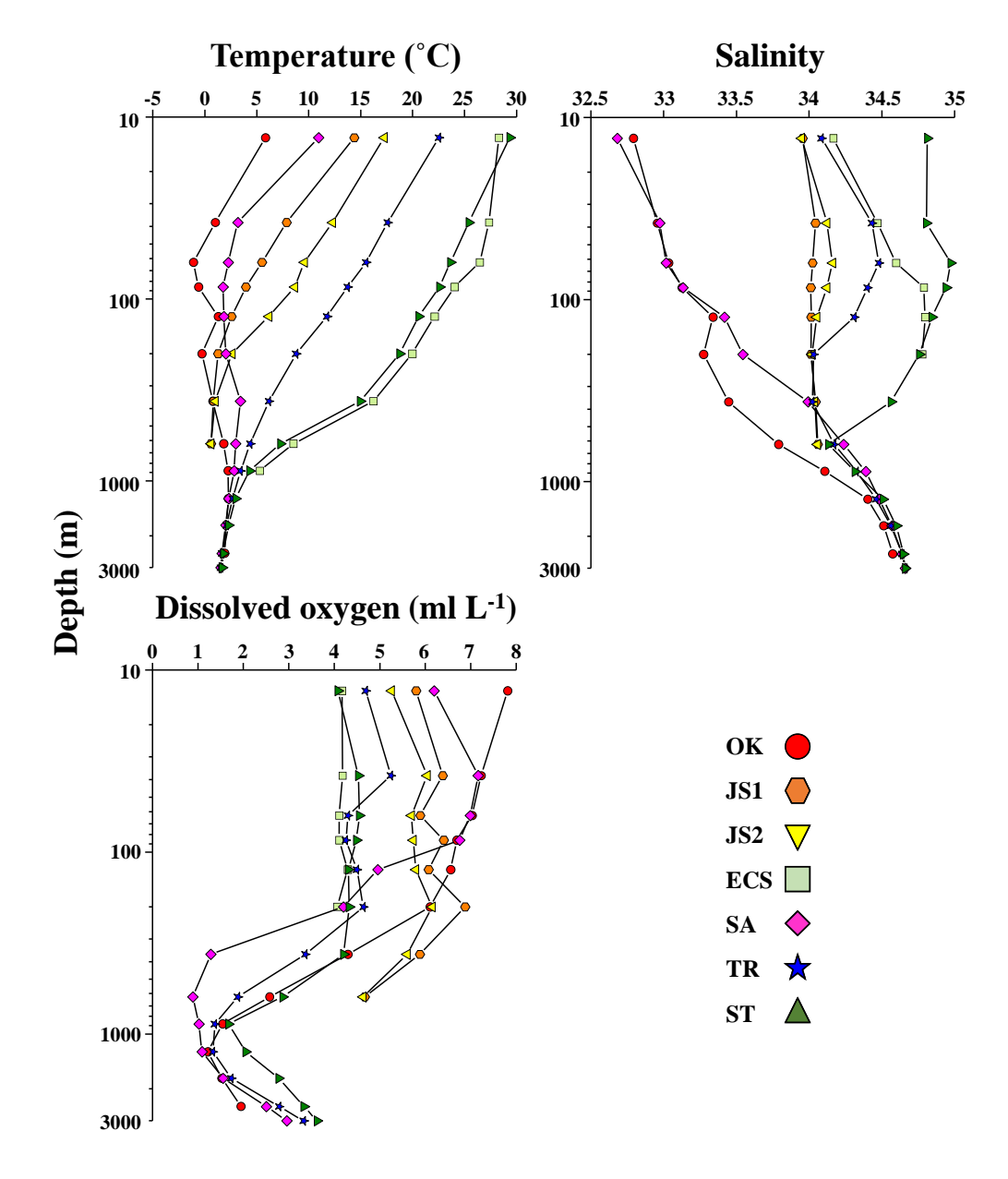


Fig. 2. Vertical changes in temperature, salinity and dissolved oxygen at the seven stations neighboring waters of Japan. OK: Okhotsk Sea, JS1: Japan Sea station 1, JS2: Japan Sea station 2, ECS: East China Sea, SA: subarctic Pacific, TR: transitional Pacific, ST: subtropical Pacific. Symbols denote mean values for the sampling depths of VMPS at each station.

uniform throughout the layers.

DO ranged between 0.85 and 7.90 ml L<sup>-1</sup> throughout the stations. Common for all stations, DO had a minimum of around 1000 m depths. For the shallower depths, especially above 200 m, DO was the highest for the subarctic (St. OK, SA), the lowest for the subtropical (St. ECS, TR, ST), then settled between them for the Japan Sea (St. JS1, JS2).

The T-S diagram at each station is shown in Fig. 3. The plotted area in the T-S diagram was greatly varied with the stations. Thus, for the subarctic (St. OK, SA), temperatures were cold and similar throughout the layer while salinities were increased with increasing depths which induced increasing density with increasing depths. While for the subtropical (St. ECS, TR, ST) and the Japan Sea (JS1, JS2), salinities were high and similar throughout the layer, but temperatures decreased with

increasing depths which provided increasing densities with increasing depths there.

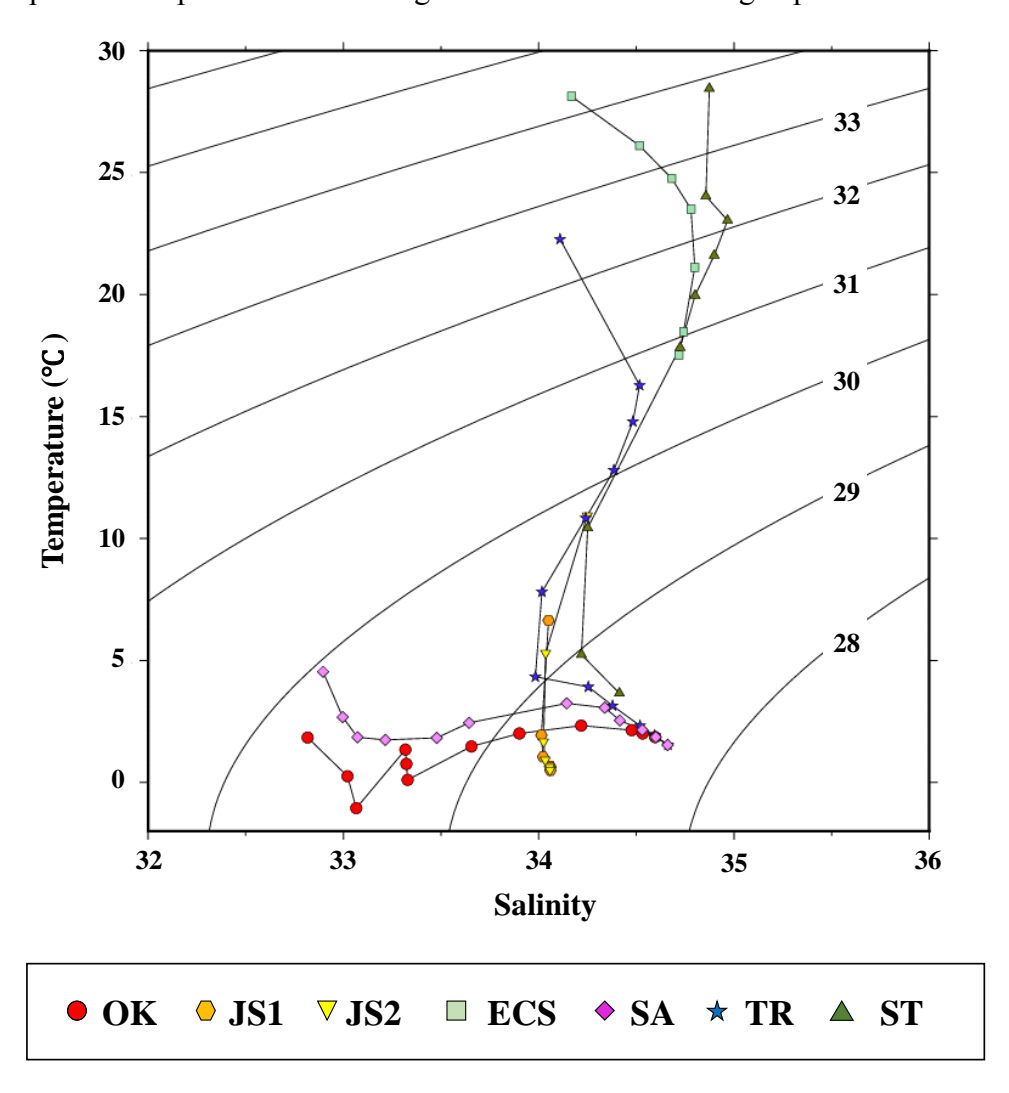


Fig. 3. T-S diagram at the seven stations neighboring waters of Japan. OK: Okhotsk Sea, JS1: Japan Sea station 1, JS2: Japan Sea station 2, ECS: East China Sea, SA: subarctic Pacific, TR: transitional Pacific, ST: subtropical Pacific. Symbols denote mean values for the sampling depths of VMPS at each station.

# 3.2. Abundance and biovolume

Zooplankton abundance (ind. m<sup>-3</sup>) and their taxonomic composition at each sampling layer based on the ZooScan measurement are shown in Fig. 4. For most of the stations, abundance was the highest near the surface layer and then decreased with increasing depths. For taxonomic composition, Calanoida was dominated and composed ca. 30% throughout the station and layers. For the 0–250 m of the subarctic stations (St. OK, JS1, JS2, SA), Cyclopoida was also dominated. For the deeper layers below 250 m of St. OK and SA and the whole layers of the subtropical stations (St. ECS and ST), Poecilostomatoida was also dominated and composed more than 30%.

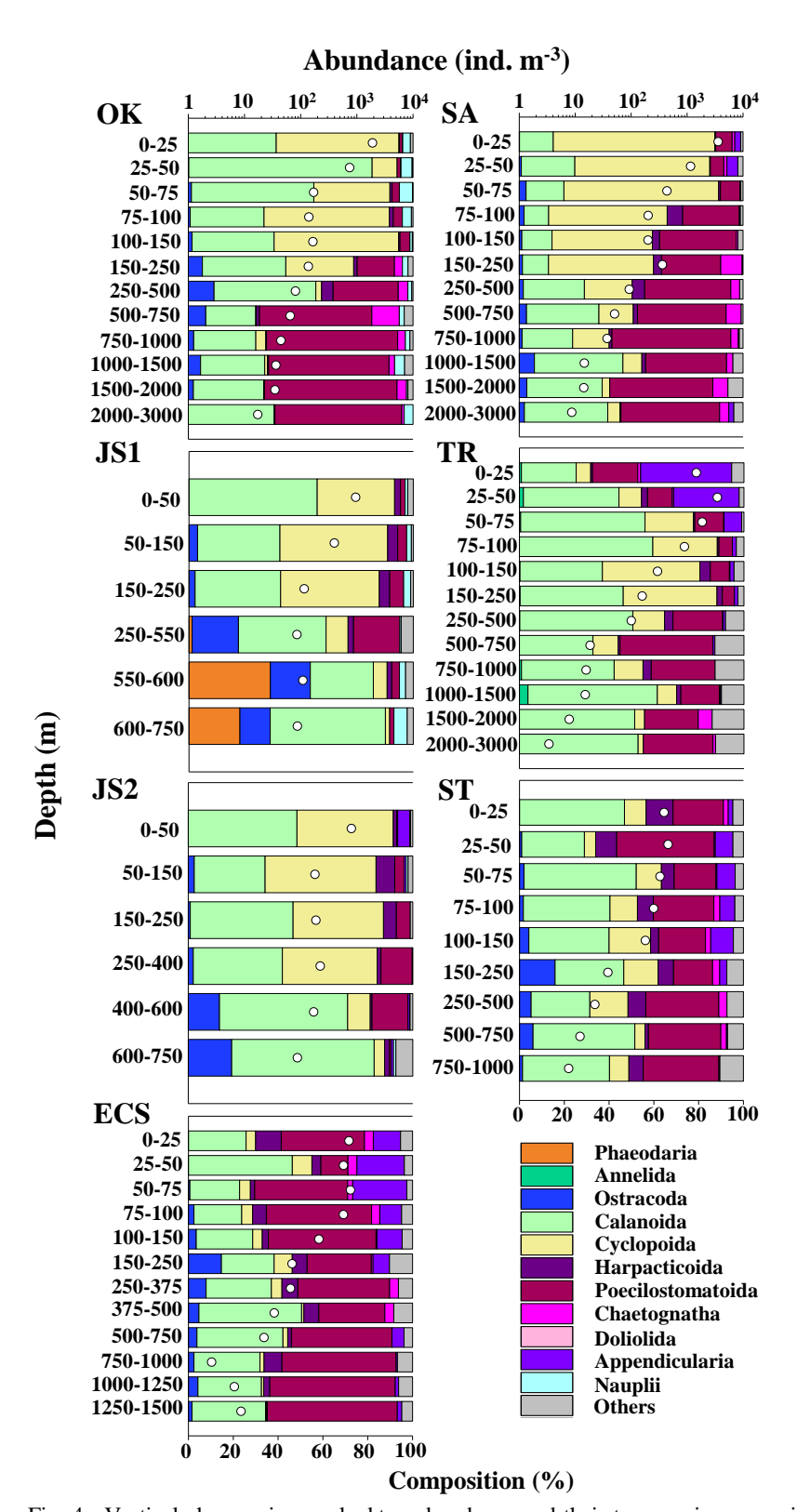


Fig. 4. Vertical changes in zooplankton abundance and their taxonomic composition at the seven stations neighboring waters of Japan. Note that abundance scales are in log-scales. OK: Okhotsk Sea, JS1: Japan Sea station 1, JS2: Japan Sea station 2, ECS: East China Sea, SA: subarctic Pacific, TR: transitional Pacific, ST: subtropical Pacific.

Zooplankton biovolume (mm<sup>3</sup> m<sup>-3</sup>) and their taxonomic composition at each layer are shown in Fig. 5. For biovolume, the sporadic high composition of Euphausiacea was seen at 50–150 m of St. JS1 and 150–250 m of St. JS2. The most dominant taxon was Calanoida. The second dominant

taxa were varied with the station: Chaetognatha (St. OK, SA, and ST), Doliolida at the deep layer of St. TR. Phaeodaria dominated the deep layer of St. JS1 which was common for the abundance at those layers.

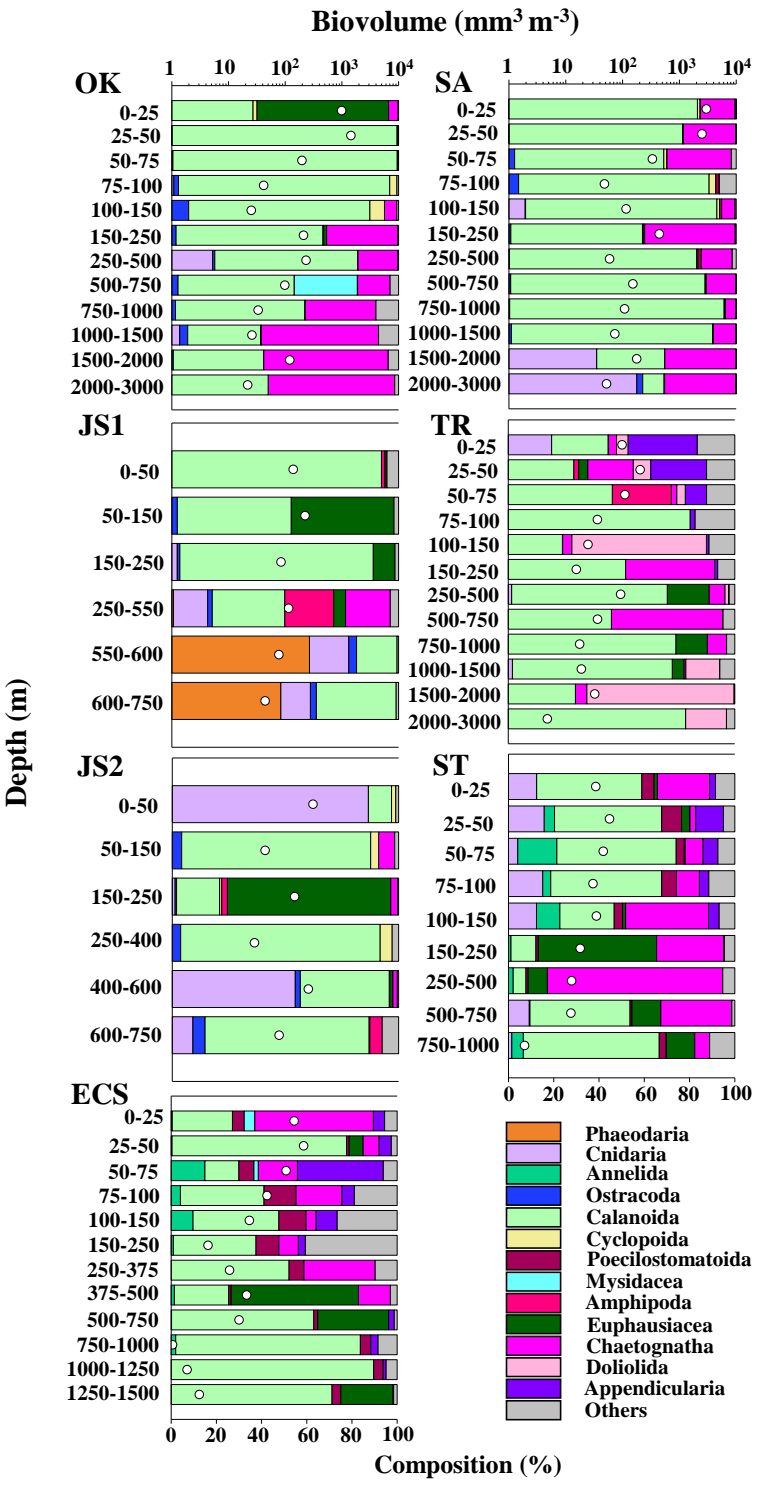


Fig. 5. Vertical changes in zooplankton biovolume and their taxonomic composition at the seven stations neighboring waters of Japan. Note that biovolume scales are in log-scales. OK: Okhotsk Sea, JS1: Japan Sea station 1, JS2: Japan Sea station 2, ECS: East China Sea, SA: subarctic Pacific, TR: transitional Pacific, ST: subtropical Pacific.

Vertical changes in zooplankton abundance and biovolume, along with the increasing depths, are shown in Fig. 6. These vertical changes were fitted to the power regressions, and their slopes and

intercepts are shown in Table 2. For abundance, significant regressions were observed for all seven stations, and their slopes were between -0.531 and -1.379 (Table 2). For the regressions on biovolume, their fittings were lower than those of the abundance considering  $r^2$  and p-values (Table 2). For two stations of the Japan Sea (JS1 and JS2), insignificant regressions were the cases. It was due to the sampling depths being limited between 0 and 750 m and the low number of stratification (six layers) within the stations. For prominent characteristics of biovolume, the sharp decreases with the magnitude at ca. 1/10 were seen at 75–100 m depths of St. OK and SA (Fig. 6b). It also should be noted that the depths corresponded with the depths observed in the intermediate cold water at these stations (Fig. 2).

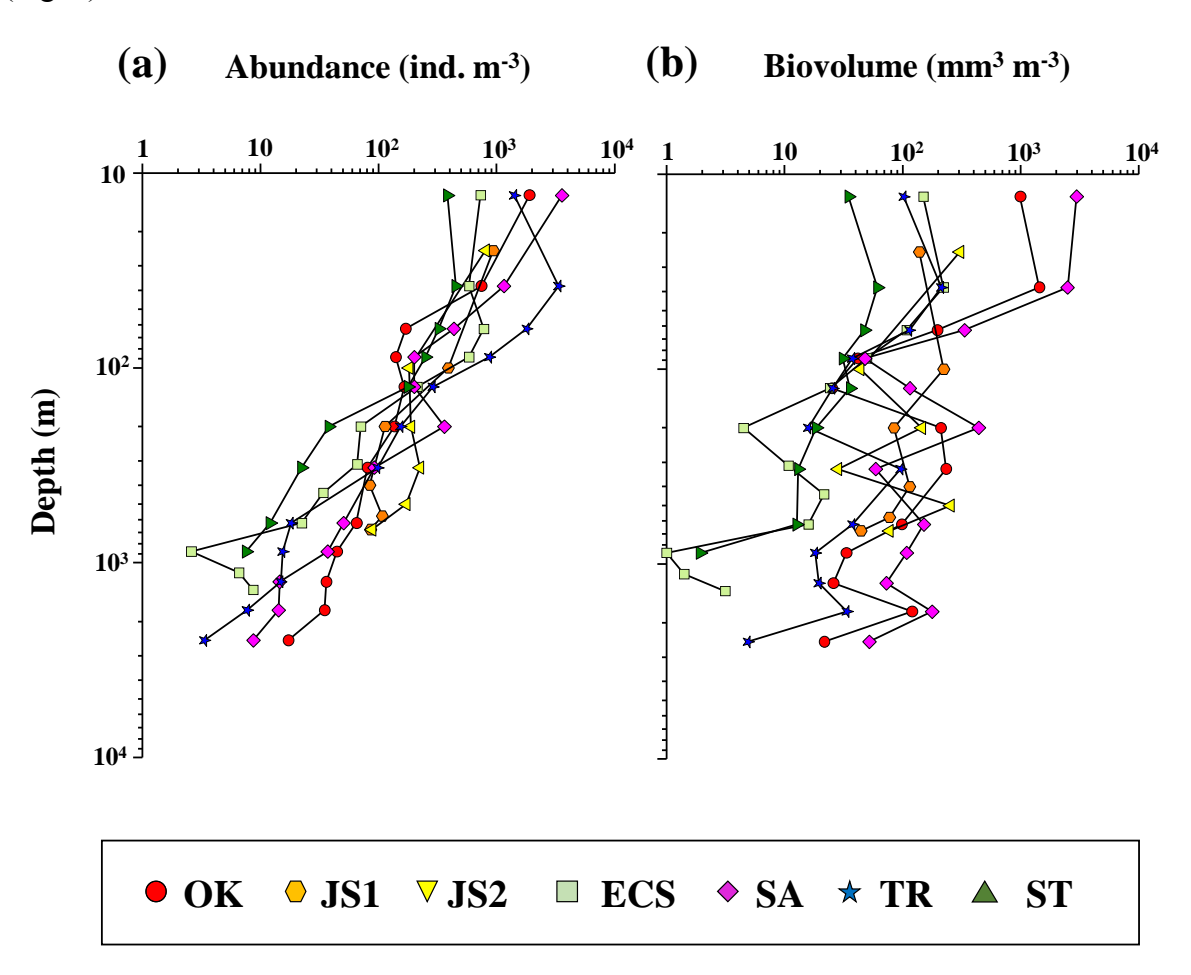


Fig. 6. Vertical changes in zooplankton abundance (a) and biovolume (b) at the seven stations neighboring waters of Japan. OK: Okhotsk Sea, JS1: Japan Sea station 1, JS2: Japan Sea station 2, ECS: East China Sea, SA: subarctic Pacific, TR: transitional Pacific, ST: subtropical Pacific.

Table 2. Regression statistics of abundance (Abu: ind. m<sup>-3</sup>) and biovolume (Bio: mm<sup>3</sup> m<sup>-3</sup>) along with depth (D: m) for the seven stations neighboring waters of Japan. As regressions, power models were used:  $\log_{10}Abu = a \log_{10}D + b$  or  $\log_{10}Bio = a \log_{10}D + b$ , where a and b were fitted constants. For details of data, see Fig. 6. \*: p<0.05, \*\*: p<0.01, \*\*\*: p<0.001, ns: not significant.

Unit	Station	a	b	$r^2$
Abun	dance			
	OK	-0.774	8.996	0.925***
	JS1	-0.755	9.204	0.909**
	JS2	-0.531	8.157	0.7839*
	ECS	-1.277	11.119	0.863***
	SA	-1.107	10.898	0.961***
	TR	-1.379	12.334	0.923***
	ST	-1.108	9.827	0.868***
Biovo	olume			
	OK	-0.586	7.940	0.466*
	JS1	-0.306	6.238	0.479ns
	JS2	-0.249	5.927	0.099ns
	ECS	-1.088	8.589	0.764***
	SA	-0.602	8.624	0.501**
	TR	-0.465	6.196	0.533**
	ST	-0.621	6.056	0.648**

As environmental factors affect the abundance and biovolume, two factors: the region and depth, were available. Results of ANCOVA applying abundance and biovolume as target variables and region and depth as dependent variables are shown in Table 3. The effects of two factors varied between the abundance and biovolume. Thus, for abundance, depth was the only environmental factor to affect, and the other factors (region and interactions of region×depth) had no effect on abundance. Since there was no effect of interactions of region×depth on abundance, the regressions of the abundance of the seven stations were not varied and treated as the regressions having the same slopes. On the other hand, the biovolume was affected by region, and other factors (depth and interactions of region×depth) had no effect on the biovolume (Table 3). This, the biovolume varied with region, and their biovolume values varied with depths smaller than those with the region.

Table 3. Results of ANCOVA on zooplankton abundance and biovolume, with the sampling depth (m) and region (station) (cf. Table 1) applied as independent variables. df: degree of freedom, SS: sum of squares.

Unit							
Parameter	df	SS	<i>F</i> -value	<i>p</i> -value			
Abundance							
Depth	1	1939593	4.841	0.032			
Region	6	2839226	1.181	0.3299			
Depth × Region	6	667003	0.277	0.9452			
Error	55	22035058					
Biovolume							
Depth	1	174728	0.84	0.3634			
Region	6	3773762	3.024	0.0126			
Depth × Region	6	899340	0.721	0.6346			
Error	55	11438501					

# 3.3. Zooplankton community

Based on abundance data, zooplankton species/taxa were classified into five groups (I–□) at a 28% similarity level, and their communities were clustered into eight groups (A–H) at a 68% similarity level (Fig. 7). Based on cluster results on species/taxa, the group I composed by main copepods such as Calanoida, Cyclopoida, and Poecilostomatoida. For the other groups, Mollusca and Doliolida (group II), Euphausiacea (group III), Phaeodaria (group IV), and Cnidaria (group V) were the major component taxa of each group.

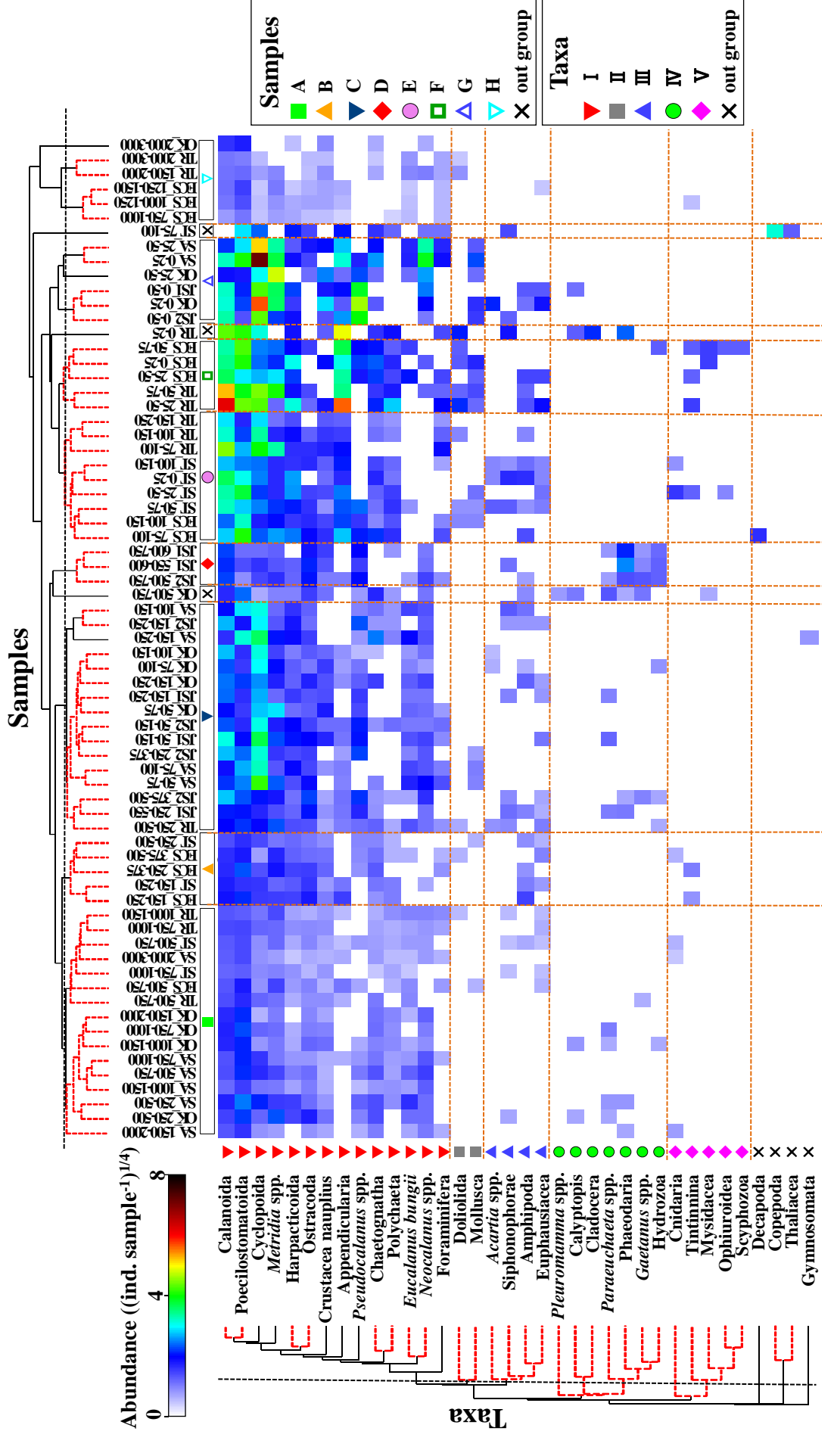


Fig. 7. Result of cluster analysis based on the mesozooplankton abundance of each sample collected from 0-3000 m strata of the seven stations neighboring waters of Japan. OK: Okhotsk Sea, JS1: Japan Sea station 1, JS2: Japan Sea station 2, ECS: East China Sea, SA: subarctic Pacific, TR: transitional Pacific, ST: subtropical Pacific. For samples, numbers after underbar represent depth layers (m)

Zooplankton communities were plotted at different locations even for the NMDS plot, and various environmental parameters (temperature, salinity, DO, depth, and latitude) had significant interaction with the plotted area of each sample in the NMDS plot (Fig. 8). From directions of each environmental variable and plotted area of each zooplankton community in the NMDS plot, following interactions were evidenced: thus, group D was seen at the high latitude, group F was seen at hightemperature regions, group G was at the high DO region/depths, and group H was seen at the deep and high salinity region and depths.

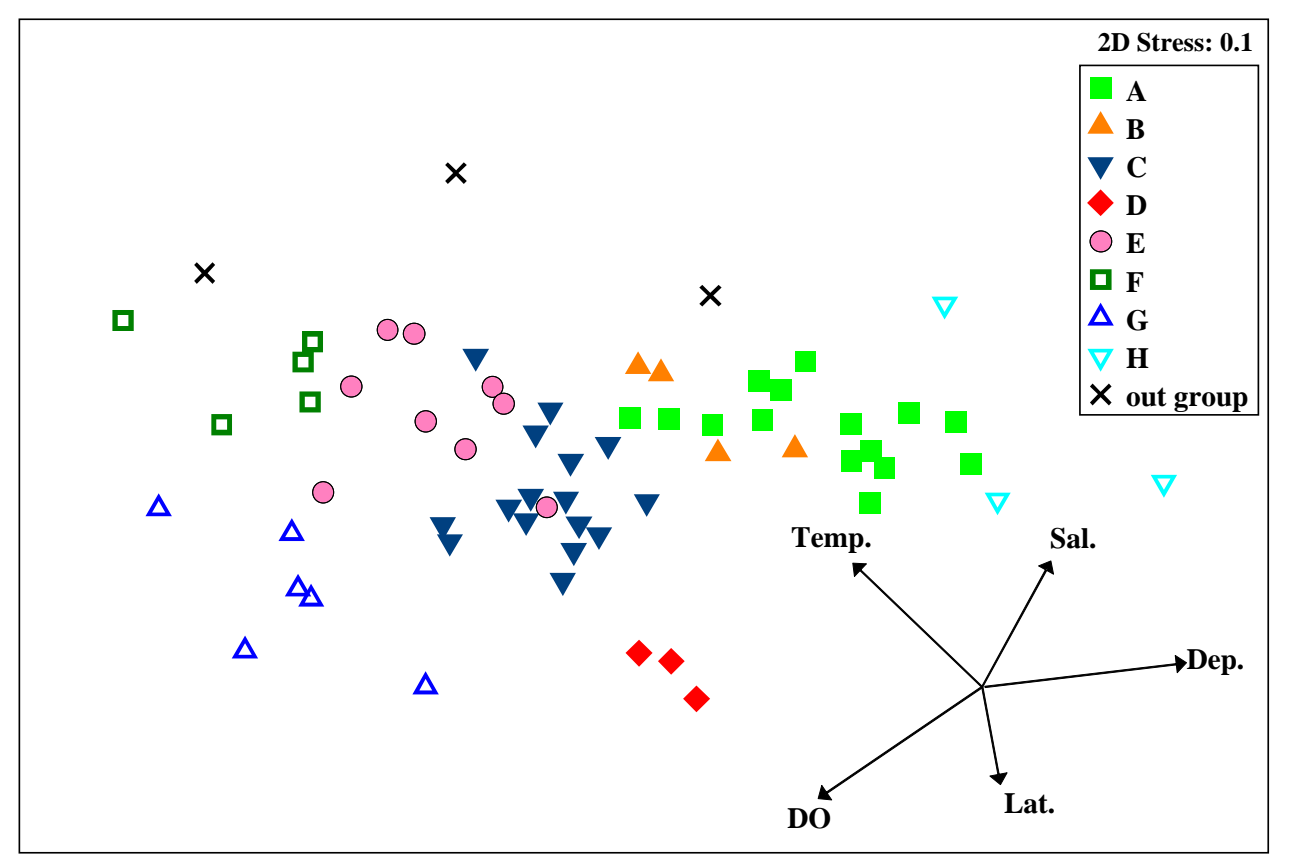


Fig. 8. Two-dimensional map by non-metric multidimensional scaling method (NMDS) of zooplankton communities specified by the depth-station complex data. Eight groups (group A-H) that clustered according to the Bray-Curtis similarity index (Fig. 7) are shown by the different symbols. Arrows indicate directions of significant environmental parameters. Lat.: latitude, Dep.: depth, Temp.: temperature, Sal.: salinity, DO: dissolved oxygen.

Results of abundance differences between zooplankton groups evaluated by one-way ANOVA and post hoc Tukey-Kramer test are shown in Table 4. Within the zooplankton species/taxa, copepods (Calanoida, Cyclopoida, and Poecilostomatoida) were dominant throughout the community. For the other zooplankton species/taxa, a specific abundant zooplankton community was present for certain zooplankton species/taxa. Thus, calanoid copepod *Metridia* spp. was abundant in the zooplankton communities of groups A, B, G, and H (Table 4). For zooplankton community group D, Phaeodaria and Ostracoda were abundant. For group F, Appendicularia was abundant, and

 $\frac{60}{295}$ 

Table 4. Mean abundance (ind.  $m^{-3}$ ) of each zooplankton taxon at eight clustered groups (A–H) identified by Bray-Curtis similarity analysis (cf. Fig. 7). The numbers in the parentheses indicate the number of samples included in each group. Differences between groups were tested by one-way ANOVA and post hoc Tukey–Kramer test. For the results of the Tukey–Kramer test, any groups not connected by the underlines are significantly different (p<0.05). -: no occurrence, \*: p<0.05, \*\*: p<0.01, \*\*\*: p<0.001, NS: not significant. For abundance, the upper three most dominant taxa/species are shown by the bold and underlines.

				Abundan	ce (ind.m <sup>-3</sup> )				one-way								
Taxa/Species	A (16)	B (5)	C (16)	D (3)	E (9)	F (5)	G (6)	H (6)	ANOVA	Tuk	ey-K	rame	test				
Phaeodaria	0.040	-	0.090	20.630	-	-	-	-	***						A	C	D
Foraminifera	0.110	0.130	0.480	0.210	2.310	4.310	3.470	0.120	*			No	t dete	cted			
Tintinnina	-	0.310	-	-	0.250	1.950	-	0.010	***					Н	Е	В	F
Cnidaria	0.030	0.020	-	-	0.730	-	-	-	NS								
Hydrozoa	0.010	-	0.060	2.090	-	0.500	-	-	***					A	C	F	D
Scyphozoa	-	-	-	-	-	0.500	-	-	NS								
Siphonophorae	0.030	-	0.440	0.490	1.150	-	0.370	-	NS								
Annelida	0.320	0.460	0.240	0.150	2.930	16.820	-	0.000	***		Н	D	C	A	В	E	F
Gymnosomata	-	-	0.030	-	-	-	-	-	NS								
Ostracoda	1.350	4.870	7.090	<u>15.900</u>	5.450	2.140	2.760	0.100	***	Н	A	F	G	В	E	C	D
Calanoida	4.330	7.750	33.430	22.840	122.740	519.060	76.340	2.080	***	Н	A	В	D	C	G	E	F
Acartia spp.	-	-	0.050	-	0.450	-	3.260	-	NS								
Eucalanus bungii	0.940	0.020	2.970	0.100	0.060	4.420	3.020	0.230	NS								
Gaetanus spp.	0.010	-	0.060	1.340	-	-	-	-	***						A	C	D
Metridia spp.	3.640	5.550	14.820	4.160	26.180	77.040	200.350	0.460	***	Н	A	D	В	C	Е	F	G
Neocalanus spp.	1.310	0.040	3.440	2.450	-	0.920	74.020	0.190	***		В	Н	F	A	D	С	G
Paraeuchaeta spp.	0.120	-	0.240	0.260	-	-	-	-	NS								
Pseudocalanus spp.	0.360	0.400	8.240	12.100	6.210	9.840	157.350	-	***		A	В	E	C	F	D	G
Cyclopoida	2.950	3.750	91.840	4.110	<u>67.140</u>	168.840	844.580	0.090	***	Н	A	В	D	Е	C	F	G
Harpacticoida	0.840	3.200	6.480	1.370	19.780	44.820	9.650	0.080	***	Н	A	D	В	C	G	Е	F
Poecilostomatoida	13.180	14.230	27.060	1.980	93.320	253.090	65.140	<u>3.770</u>	***	D	Н	A	В	C	G	Е	F
Mysidacea	-	-	-	-	-	2.050	-	-	***								
Amphipoda	0.010	1.360	0.310	0.100	1.480	1.930	0.690	-	*			Not c	letect	ed			
Euphausiacea	0.030	0.290	0.250	-	0.450	3.570	2.320	0.010	*		Н	A	C	В	Е	G	F
Calyptopis	0.040	-	-	-	-	-	0.230	-	NS								
Chaetognatha	1.200	1.300	2.880	-	4.510	18.890	10.500	0.070	***	D	Н	A	В	C	E	G	F
Doliolida	0.000	0.020	0.010	-	0.230	5.500	-	0.090	**			A	С	В	Н	Е	F
Appendicularia	0.120	1.280	0.640	0.310	21.280	304.220	35.650	0.050	***	Н	A	D	С	В	Е	G	F
Ophiuroidea	-	-	-	-	0.080	0.500	-	-	NS								. —
Mollusca	0.010	0.030	0.130	-	0.310	3.130	7.060	-	***			A	В	E	E	F	G
Decapoda	-	-	-	_	0.790	-	-	-	NS			_					
Crustacean nauplius	0.480	1.120	2.200	2.990	4.160	5.510	21.870	0.330	***	Н	A	В	С	D	Е	F	G
Total	31.46	46.13	203.47	93.59	382.01	1449.56	1518.63	7.68	***	Н	A	В	D	С	Е	F	G

Occurrences (geographical and vertical distribution) of each zooplankton community are shown in Fig. 9. Each group occurred at consecutive regions and depths. Occurrences of each zooplankton group were classified into two regions: thus, the subarctic stations (St. OK, JS1, JS2, SA) and transitional and subtropical stations (ECS, TR, ST). For the subarctic stations, group G was seen at the shallower 0–50 m depths, then group C was seen at 50–500 m, and group A was dominated below that layer (>500 m) (Fig. 9). As regional special characteristics, the group D was only seen for the deep layer (>500 m) of the Japan Sea, and it should be noted that the depths were corresponded with the occurrence of the Japan Sea Proper Water (Fig. 2). For the transitional and subtropical stations, group E and F were seen at the shallower 0–300 m depths, and group B was seen for 200–500 m depths, then groups A and H was occurred for the deepest layer (>500 m) (Fig. 9).

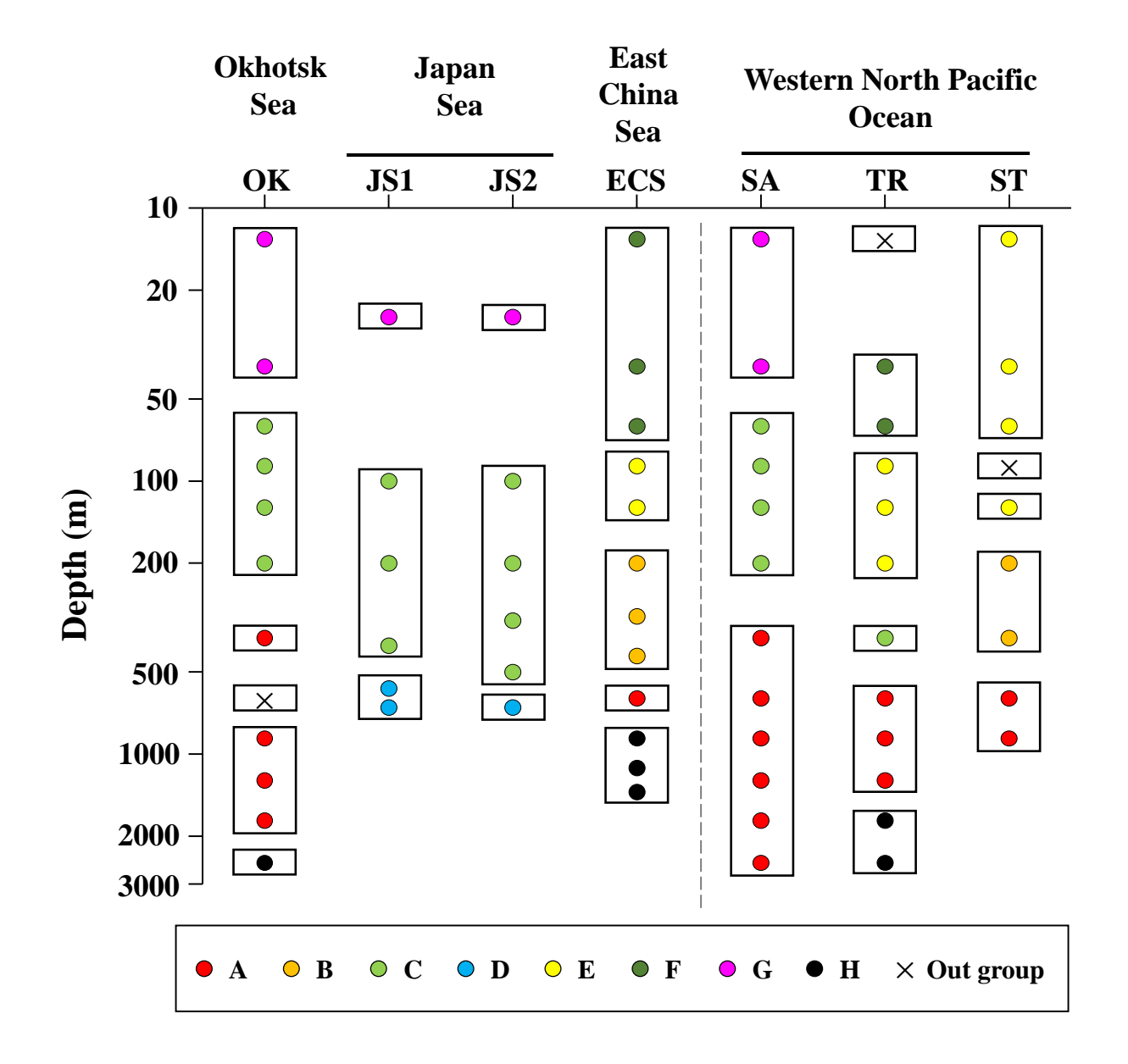


Fig. 9. Spatial and vertical distribution of zooplankton community groups identified by Bray-Curtis similarity index (cf. Fig. 7). Sampling depth at each station is shown by the symbols. Note that depth scale is in log-scale. OK: Okhotsk Sea, JS1: Japan Sea station 1, JS2: Japan Sea station 2, ECS: East China Sea, SA: subarctic Pacific, TR: transitional Pacific, ST: subtropical Pacific.

# 3.4. Zooplankton NBSS and size diversity

Results of NBSS based on zooplankton biovolume at each sampling layer of the seven sampling stations are shown in Fig. 10. Common for the whole region and depths, biovolume changes along with the sizes were generally smooth, and significant NBSS was obtained for all the samples. The vertical changes in slopes and intercepts of NBSS and size diversity of each sample are shown in Fig. 11. Slopes of NBSS were zero or positive for the surface layer (0–50 m) of the subarctic stations (St. OK and SA). It also should be noted that the prominent decrease of the slope, the intercept of NBSS, and size diversity were observed for subsequent 100–150 m depths. As the common patterns observed for the whole region, the three parameters: slope and intercept of NBSS,

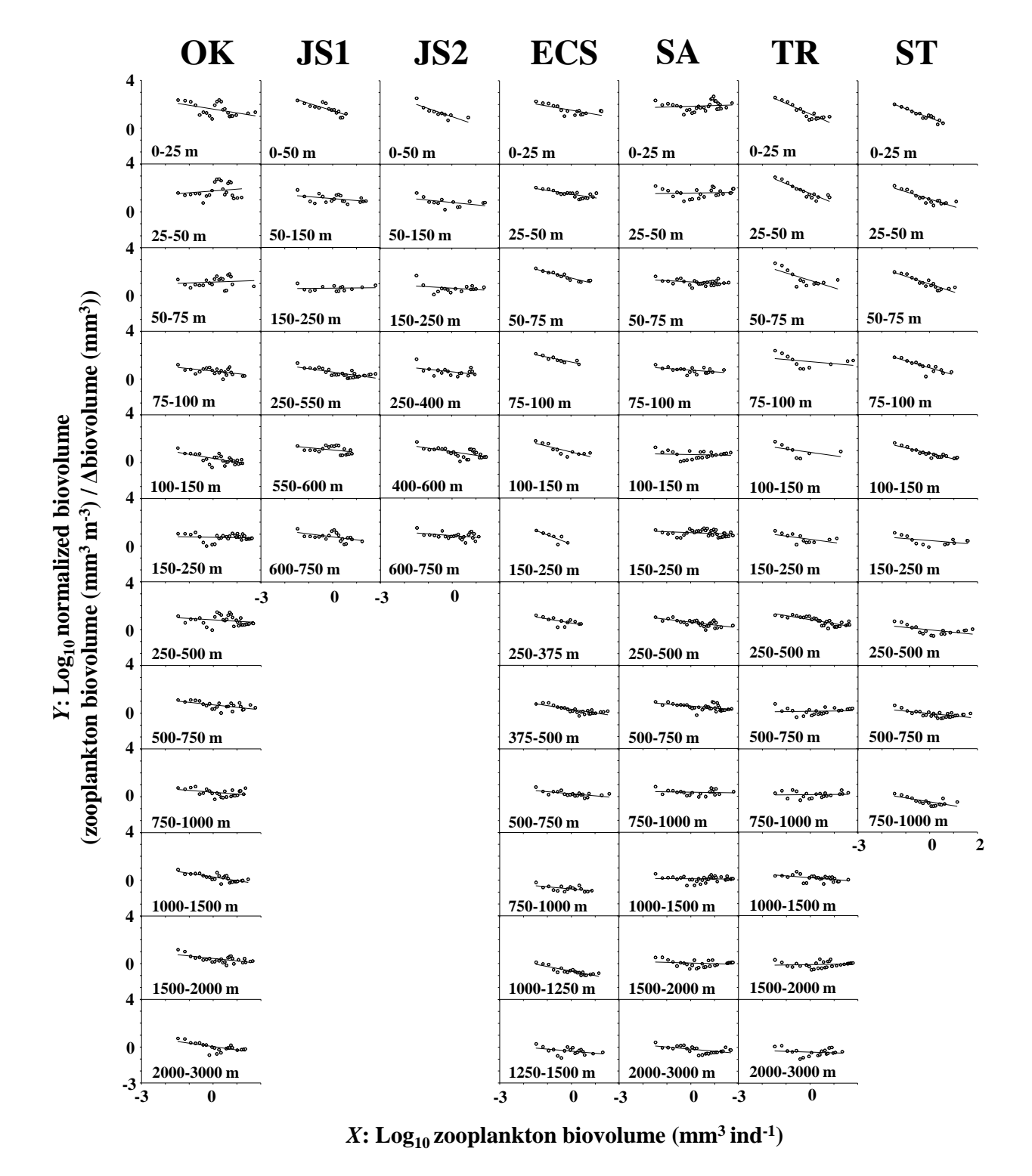


Fig. 10. Vertical changes in normalized biovolume size spectra (NBSS) at various depth strata of the seven sampling stations neighboring waters of Japan. Note that NBSS regressions are highly significant ( $r^2$ =0.15-0.9, p<0.05) for all sampling depths. OK: Okhotsk Sea, JS1: Japan Sea station 1, JS2: Japan Sea station 2, ECS: East China Sea, SA: subarctic Pacific, TR: transitional Pacific, ST: subtropical Pacific.

and size diversity showed great changes around 150–500 m depths. Thus, above 150–500 m depths, the slopes of NBSS were steep, intercepts of NBSS were high, and size diversity was low, while the moderate slope of NBSS and low intercept of NBSS, and high size diversity were the cases of below 150–500 m depths (Fig. 11). Such vertical changes in slope and intercept of NBSS, and size diversity

 were prominent, especially at St. TR, ST, and ECS. On the other hand, the slope of NBSS was moderate, even in the surface layer of St. SA.

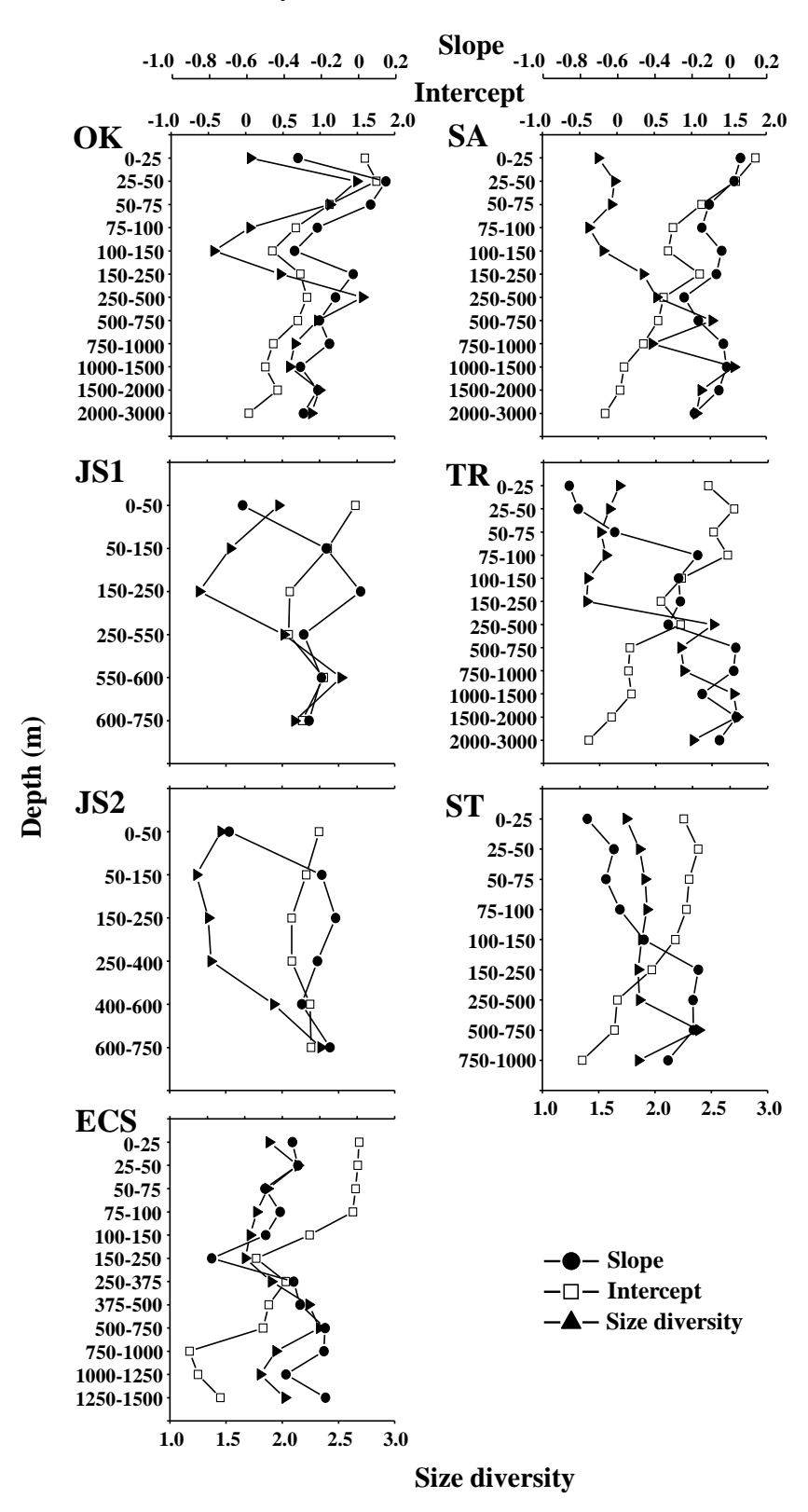


Fig. 11. Vertical changes in slope and intercept of the normalized biovolume size spectra (NBSS) and size diversity at various depth strata of the seven sampling stations neighboring waters of Japan. OK: Okhotsk Sea, JS1: Japan Sea station 1, JS2: Japan Sea station 2, ECS: East China Sea, SA: subarctic Pacific, TR: transitional Pacific, ST: subtropical Pacific.

Scatter plots of the three parameters: slope and intercept of NBSS, and size diversity are shown in Fig. 12. Throughout the station, it was marked that the slopes of NBSS at 200–1000 m and 1000–3000 m depths were moderate and plotted at the limited areas in the scatter plot. While the plotted area of the NBSS slope at 0–200 m depth was broad and varied with the station. The steep slopes of NBSS were seen for the subtropical stations, while moderate slopes of NBSS were the cases of the subarctic stations.

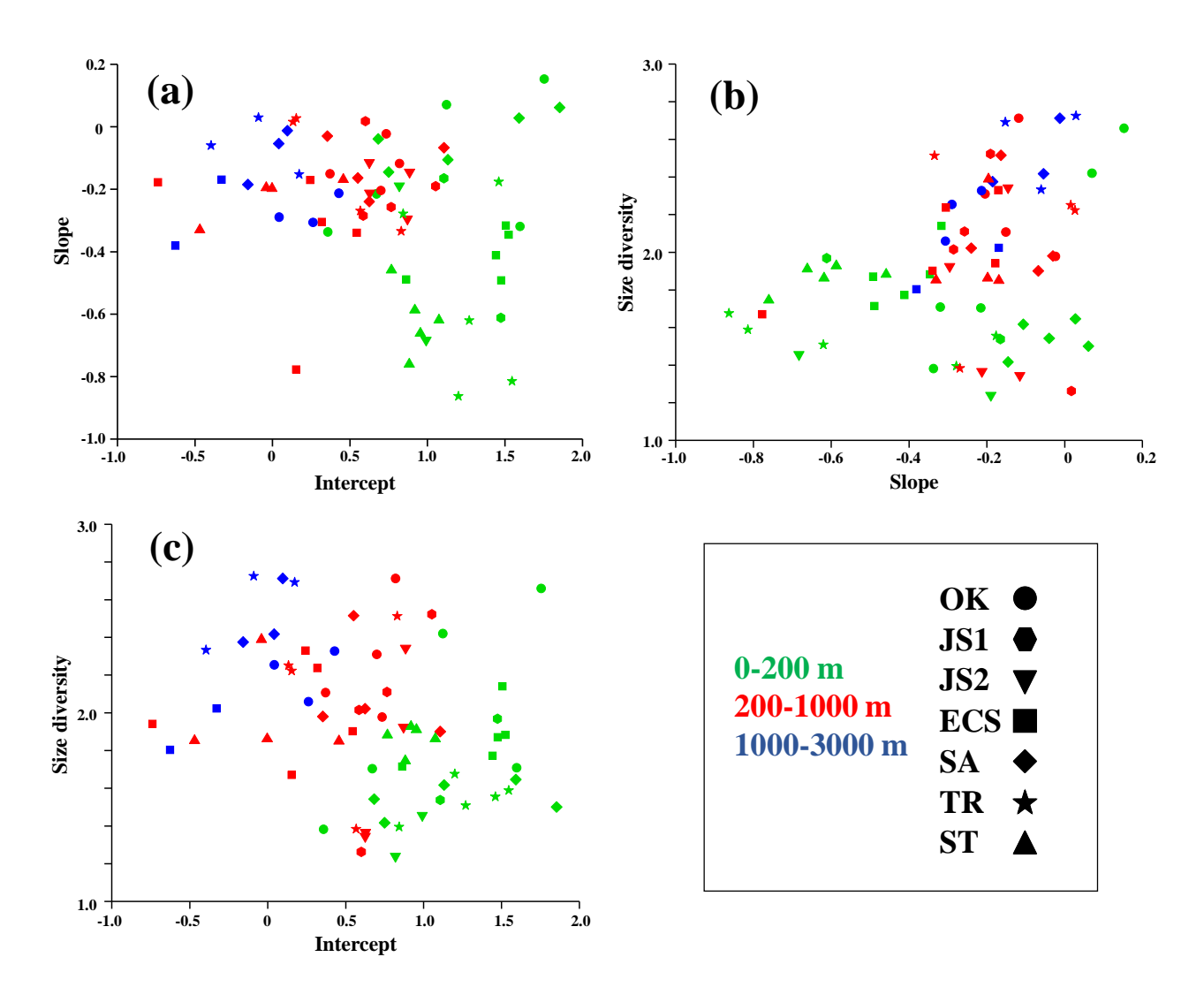


Fig. 12. Scatter plots between slope and intercept of NBSS (a), size diversity and slope of NBSS (b), and size diversity and intercept of NBSS (c) at seven stations neighboring waters of Japan. OK: Okhotsk Sea, JS1: Japan Sea station 1, JS2: Japan Sea station 2, ECS: East China Sea, SA: subarctic Pacific, TR: transitional Pacific, ST: subtropical Pacific. Differences in colors represent sampling depths (0-200, 200-1000, and 1000-3000 m).

Results of GAM analysis applying target variables as slope and intercept of NBSS, and size diversity and explanation variables as environmental parameters: depth, temperature, and salinity are shown in Fig. 13. The slope of NBSS had a significant effect by temperature, and warm conditions induced steep slope, while cold conditions implied moderate slope. The intercept of NBSS had

significant interactions with depth and salinity. For shallower depths, the intercept of NBSS was high, while the low intercept of NBSS was the case for the deep layers. As an effect of salinity, the intercept of NBSS was high at the low salinity conditions, while the low NBSS intercept was in the cases of the high salinity conditions. Size diversity had significant interaction with the depth. Thus, the size diversity was low at the shallower depths, while was increased with increasing depths. This depth-related interaction of size diversity was highly significant (p<0.001).

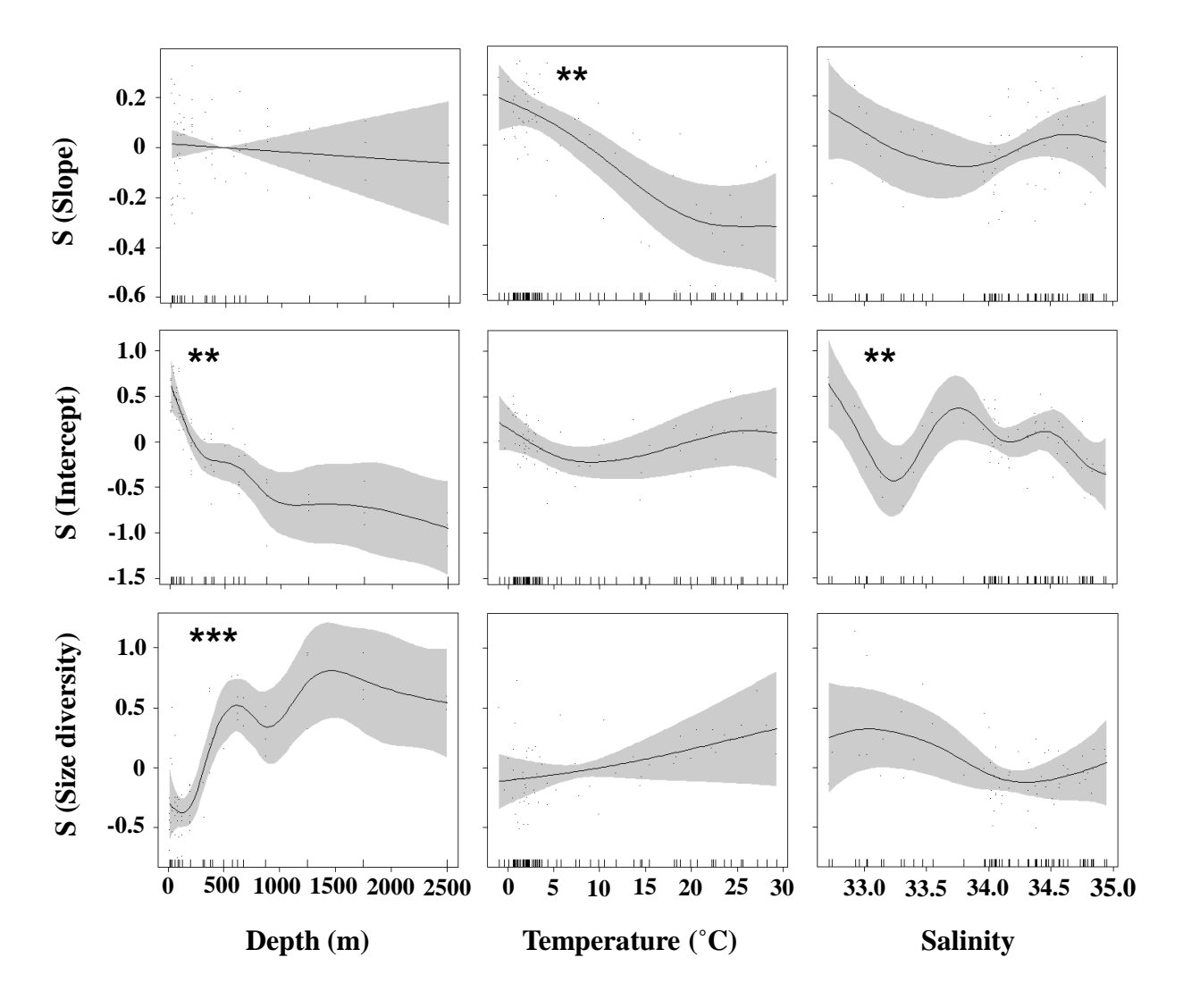


Fig. 13. Result of GAMs based on anomalies of the slope and intercept of NBSS and size diversity with environmental parametrs (depth, temperature and salinity). \*\*: p<0.01, \*\*\*: p<0.001

Results of inter-group differences in slope and intercept of NBSS and size diversity tested by one-way ANOVA and post hoc test (Tukey-Kramer) are shown in Table 5. For the slope of NBSS, the groups E and F observed at the epipelagic zones of the subtropical stations (Fig. 9) were evaluated to have steep slopes. As groups having a high intercept of NBSS, groups F and G were prominent. These two groups were seen at surface 0–75 m of the subtropical (group F) or subarctic (group G)

63 64 65

regions. As groups having high size diversity, groups A and D were present. These two groups were the deep-sea communities observed below 500 m depths. Thus, the three indices on the zooplankton size: slope and intercept of NBSS, and size diversity varied greatly with the zooplankton community.

#### 4. Discussion

### 4.1. Abundance and biovolume

For abundance, three orders of Copepoda (Calanoida, Poecilostomatoida) contributed Cyclopoida, and high compositions. Within them, Calanoida contains various feeding modes: particulate feeders, detritivores, and carnivores, and they have important roles as the mediator of energy transfer to the higher trophic level and vertical material flux (Mauchline, 1998). For the small-sized copepod, Cyclopoida was dominated at 0–250 m of the subarctic stations (Fig. 4). Cyclopoida feeds mainly on microzooplankton such as ciliates and are considered to have an important role in the transfer of the microbial production to the higher trophic levels (Nishibe et al., 2010). On the other hand, the other small-sized copepod Poecilostomatoida is considered to be a detritivore that feeds on detritus and is attached to the marine snow (Turner, 2004). Poecilostomatoida was abundant below 250 m of the subarctic stations and the whole water column of the subtropical stations. The dominance of Poecilostomatoida at the deep layer of the subarctic Pacific is well documented (Yamaguchi et al., 2002a; Nishibe and Ikeda, 2004). For the subtropical Pacific, attachment of Poecilostomatoida on the discarded appendicularian house is reported (Nishibe et al., 2015).

For biovolume, add to Calanoida, sporadic high composition was seen for Euphausiacea (Fig. 5). The dominant species of Euphausiacea in the western North Pacific, and their marginal seas are reported to be Euphausia pacifica and Thysanoessa spp. both is reported to perform diel vertical migration (DVM) (Iguchi et al., 1993; Taki, 2006, 2011). Stations observed the occurrence of Euphausiacea above 250 m depths corresponded with the samplings conducted at night (Table 1). For the other prominent taxa in biovolume: Phaeodaria, their

5. Inter-group differences in zooplankton size relataed variables (slopes and intercepts of NBSS and size diversities) evaluated for zooplankton

samples collected from 0-3000 m depths of the seven sampling stations at neighboring waters of Japan. For details of the location of the stations and distribution of each zooplankton community clustered by the zooplankton abundance data, see Figs. 1 and 9, respectively. For detailed data of NBSS and size diversity see Figs. 10 and 11, respectively.	ted from ( each zoop ity see Fig	0-3000 m columbiants of the colu	lepths of th ommunity c 11, respectiv	e seven sar lustered by vely.	npling stat the zoopl	ions at nei ankton abu	ghboring w ndance dat	aters of Jap a, see Figs.	seven sampling stations at neighboring waters of Japan. For details of the location of the stations and stered by the zooplankton abundance data, see Figs. 1 and 9, respectively. For detailed data of NBSS 13.	s of the loca ctively. For	tion deta	of the	stat lata o	ions of NF	and SSS
Z	Cooplanktor	Zooplankton community group	y group						one-way						
Parameters	A (16)	A (16) B (5) C (16)	C (16)	D (3)	E (9)	F(5)	D (3) E (9) F (5) G (6) H (6)	(9) H	ANOVA	Tukey-Kramer test	mer t	sst			
NBSS Slope	-0.143	-0.358	-0.153	-0.198	-0.458	-0.518	-0.229	-0.175	* * *	F E B G D H C A	3 G	D	Н	C	Α
NBSS Intercept 0.224	0.224	0.295	0.789	0.901	0.984	1.465	1.544	-0.356	* * *	H A B C D E F G	C	D	E	F	G
Size diversity 2.310	2.310	1.904	1.698	2.325	1.692	1.798	1.823	2.180	* * *	E C F G B H A D	, G	В	Н	Α	D
													i		

 $_{6407}^{60}$ 

62

63 64 65 dominance at the deeper layer of the Japan Sea is reported to be due to the dominance of *Aulographis japonica* in the cold Japan Sea Proper Water (Nakamura et al., 2013).

To express the depth decrease of zooplankton abundance and biomass, various regressions such as an exponential model ( $\log Y = a \ Depth + b$ ), power model ( $\log Y = a \ Depth + b$ ), and regression with an intercept at 100 m ( $Y = Y_{100} \ (Depth/100)^b$ ) are present where Y is abundance or biomass, and  $Y_{100}$  is the intercept value at 100 m depth (Yamaguchi et al., 2002a, 2002b, 2004, 2005). In the present study, we applied power regression to both abundance and biovolume. For the comparable study, Yamaguchi et al. (2002a) applied power regressions to express depth-decreasing rates of Copepoda in the western subarctic Pacific and reported that the slope (a) of the regression is steep for abundance ranged at -1.41- -1.52, while is moderate for biomass ranged at -1.10 - -1.32. The steep slope of the regression (=rapid decrease with increasing depth) of abundance than that of biomass (biovolume) was also observed in this study (Table 2).

As prominent characteristics in biovolume, rapid decrease at the cold intermediate water at St. OK and SA was marked. The cold intermediate water is brine water that originated during ice-forming last winter and is characterized by extremely cold (<0°C) and the development of strong pycnocline (Takizawa, 1982). At the intermediate cold water, the DVM of zooplankton is prevented, and the decrease of zooplankton biovolume at that layer has been well documented (Yamaguchi, 2015). These factors may induce an abrupt decrease of biovolume at intermediate cold water observed for St. OK and SA (Figs. 5, 6b).

For the decreasing rates with depth increasing, taxonomic differences are present in the plankton biomass, and the decreasing rates are more rapid for the higher trophic level organisms than those of the lower trophic level (Yamaguchi et al., 2002b, 2004). On the other hand, little attempt has been made to the differences in the unit (abundance or biomass [biovolume]) depth-related decreasing rate. In this study, the depth-related decreasing rate and intercept of abundance were similar throughout the stations. This result in abundance is greatly varied with the general patterns of zooplankton biomass: depth-decreasing rates are similar but intercepts vary (Vinogradov, 1968; Table 3 of this study). These differences would be due to the differences in the applied unit (abundance or biomass [biovolume]). As a comparable study, Yamaguchi et al. (2015) conducted depth-decreasing rates of Copepoda of 0-2615 m depths based on the vertically stratified samples collected at 16 stations covering tropical to subarctic regions (0° to 56°N in latitude) of the North Pacific. Through such a comprehensive study, the abundance of Copepoda decreases with increasing depth throughout the stations, but differences in regressions have not been observed (Yamaguchi et al., 2015). Thus, while the scarcity of information compared to the biomass, the depth-related decreasing rate and intercept of zooplankton abundance seem to be similar throughout the whole North Pacific and also the marginal seas.

 For biovolume, regional (station-to-station) differences were prominent, while decreasing with increasing depths were minor (Table 3). These facts correspond that the biomass decreasing rates with depth are similar throughout the regions, while their regional differences in intercept at the surface layer continue throughout the depths (Vinogradov, 1968; Yamaguchi et al., 2005). These phenomena have been interpreted that the origin of the energy for zooplankton starting from primary productivity occurring at the sea surface. Thus, the regions with high productivity and high biomass at the surface layer contain high values of both even in the deep layer, while the regions with low productivity and biomass at the surface layer have low values of both in the deep layer. Through the biogeochemical amounts and fluxes quantification studies in the subarctic and subtropical Pacific, most of the parameters are varied at two-fold regional differences; however, the mesozooplankton biomass is reported to be 10 times higher for the subarctic than that in the subtropical region (Steinberg et al., 2008b; Kitamura et al., 2016; Honda et al., 2017). Thus, the results on zooplankton biovolume in this study (regional differences were prominent and high in the subarctic region) are well corresponded with the results of the regional comparison study between the subarctic and subtropical Pacific.

# 4.2. Zooplankton community

This study treats zooplankton from the sea surface down to 3000 m at seven stations covering the subarctic and subtropical Pacific and their three marginal seas. Because of the study targeting broader region and depth, zooplankton community was classified into eight groups (Fig. 7). For separation of the zooplankton group, various environmental parameters have affected (Fig. 8). For instance, the oppose directions of DO and depth in the NMDS panel are interpreted that the DO was higher at the shallower depths (Fig. 2). For the zooplankton groups observed for the high DO regions, group F was seen for the warm sea surface of the subtropical region, and group G was seen for the cold surface layer of the subarctic region (Fig. 9). The same directions of depth and salinity in NMDS panel are interpreted that the salinity was high for deeper depths of most of the stations (Fig. 2). The zooplankton groups A and H which observed for high depth values in NMDS panel were restricted to deep layers (Fig. 9). Thus, plotted areas of each zooplankton group and directions of environmental parameters in NMDS are well corresponded with the regional and vertical distributions of each zooplankton group.

For the numerous dominant species, except for the predominant orders of Copepoda (Calanoida, Cyclopoida, and Poecilostomatoida), *Metridia* spp., the large-sized calanoid copepod genus, were abundant for the zooplankton groups A, B, G, and H (Table 4). Within these groups, group G was seen for the surface layers of the subarctic Pacific, Japan Sea, and Okhotsk Sea (Fig. 9). Metridia is known to perform DVM (Padmavati et al., 2004) and is dominated by *M. okhotensis* in

 the Okhotsk Sea (Yamaguchi, 2015; Arima et al., 2016), *M. pacific*a in the Japan Sea (Hirakawa and Imamura, 1993), and *M. okhotensis* and *M. pacifica* in the subarctic Pacific (Padmavati et al., 2004; Takahashi et al., 2009). The boreal large-body-sized copepod species are known to transport to the deeper layers of the transitional and subtropical regions through the submergible cold-water Oyashio (Omori and Tanaka, 1967; Kobari et al., 2008). It also noted the dominance of the deep-sea *Metridia* species (*M. venusta*) for the deep layer of the lower latitude (<30°N) (Yamaguchi et al., 2015). Thus, in the transitional and subtropical regions, the groups dominated by *Metridia* spp. (groups A, B, H) were seen only for the deeper layers.

For the other zooplankton groups, which were dominated by the specific zooplankton taxa/species, group D was dominated by Phaeodaria and Ostracoda (Table 4). The group D was seen for the deeper layers of the Japan Sea, which is composed of the cold Japan Sea Proper Water (Fig. 9). For the Japan Sea Proper Water, the dominance of the large-sized Phaeodaria: *A. japonica* has been well documented and their biomass is reported to the next to the copepods at these layers (Nakamura et al., 2013). For the Japan Sea Proper Water, the dominance of the ostracod *Conchoecia pseudodiscophora* has also been reported (Ikeda, 1990; Ikeda and Imamura, 1992). Thus, such a specialized zooplankton community in the cold Japan Sea Proper Water is well confirmed in this study.

For the other zooplankton groups dominated by the specific zooplankton taxa, group F, dominated by Appendicularia, was seen for the surface layers of the ECS and TR (Table 4, Fig. 9). Appendicularia performs filter feeding on small-sized particles in pico- and nano-sizes, then asexual reproduction, and is known to show outbreak at the surface layer of the transitional region (Yokoi et al., 2008). To make filter feeding, Appendicularia creates "house" frequently, and Poecilostomatoida is known to attach to the discarded houses of Appendicularia and utilized as feeding and living places termed "microcosm" (Nishibe et al., 2015). For zooplankton group F, dominances of Appendicularia and Poecilostomatoida were seen (Table 4). These facts suggest that Appendicularia dominated the zooplankton communities at surface layers of ECS and TR to feed on the small-sized particles, then Poecilostomatoida would attach on the discarded appendicularian houses, thus dominating such microbial loops at those layers.

Through this study, geographical and vertical distribution of zooplankton communities from the sea surface to the deep sea, including subarctic to subtropics of the western North Pacific (Fig. 9). For this region, such a vertical sectional distribution of the communities has been reported for the pelagic copepods (Yamaguchi et al., 2015) and chaetognaths (Ozawa et al., 2007). Within them, copepod communities were separated by surface and deep sea vertically and by subarctic and subtropics horizontally (Yamaguchi et al., 2015), which corresponds with this study well. For chaetognaths, their deep-sea communities have been reported to be the same through the Bering Sea

 to the subtropics, while those in the Japan Sea have been reported to be greatly varied from the other regions (Ozawa et al., 2007). The great differences in the zooplankton community of the deep sea of the Japan Sea characterized by the Japan Sea Proper Water were observed in this study (Fig. 9). It is interpreted that the basin area of the Japan Sea is deep (maximum at 3700 m and mean 1350 m), while depths of the connection strait with the other outer oceans are shallow (<130 m), which induces disconnection of the waters in the deep layer with the neighboring North Pacific, East China Sea, and Okhotsk Sea, and forming the Japan Sea Proper Water, and presence of the specialized deep-sea fauna has been reported (Zenkevitch, 1963; Vinogradov, 1968).

# 4.3. NBSS and size diversity of zooplankton

We measured slopes and intercepts of NBSS and size diversity of all the treated samples in this study. Theoretically, the slopes of NBSS have a negative value (e.g. low biomass at the large-sized higher trophic organisms), and the value: -1 has been considered for the NBSS slope under the stable marine ecosystems (Moore and Suthers, 2006; Suthers et al., 2006; Zhou, 2006; Zhou et al., 2009). On the other hand, in this study, NBSS slopes had positive values for the limited stations/depths: 25–75 m of OK and 0–75 m of SA (Fig. 10). These facts derived from higher biomass of the large-sized zooplankton at these stations/depths. These stations/depths were belonging groups C and G in the zooplankton community mentioned before (Fig. 9). The groups C and G were characterized by the dominance of the large-body-sized copepod *Neocalanus* spp. (Table 4). These facts suggest that the positive slopes of NBSS of these stations/depths may be due to the smaller size ranges of the treated zooplankton, as pointed out for the zooplankton community in the eastern North Pacific by Kwong and Pakhomov (2021). Since we have abundance and biovolume data of each taxon, added to slopes and intercepts of NBSS, we can discuss the causes of the specialized or anomalous NBSS values in detail.

The slopes of NBSS observed in this study were at -0.143– -0.51 for the mean values of each zooplankton community (Table 5). Based on the same cruise of this study, NBSS analyses by OPC have been made on zooplankton samples collected from 0–150 m using 335 μm mesh NORPAC net (Sato et al., 2015). Through this study, the NBSS slopes have been reported as –0.90 for the areas dominated by large-sized copepod *Neocalanus* spp. and as -1.11– -1.24 for other regions such as subtropical Pacific (Sato et al., 2015). On the other hand, the samples of this study were collected by the vertically stratified samplings of VMPS down to 3000 m equipped with a smaller mesh of 63 μm, then measured by ZooScan. Thus, greater differences were available between the two studies (Sato et al., 2015 and this study) in terms of the target depth (0–150 m vs. 0–3000 m), applied mesh size (335 μm vs. 63 μm), and used instruments (OPC vs ZooScan).

The differences in mesh sizes of the plankton net would provide differences in net clogging

 or filtering efficiencies. However, the filtering efficiencies measured by the flowmeter reading were high (>85%) for both mesh sizes (Electronic Supplement 1). Thus, the differences in net filtering efficiency are not considered to provide differences in NBSS slopes between the two studies (Sato et al., 2015 and this study). Since this study applied smaller mesh sizes (63  $\mu$ m), it may allow us to collect smaller-sized zooplankters and broader target size ranges for NBSS analysis and then induce steeper slopes of NBSS than those quantified by the large mesh size (335  $\mu$ m) samples. But the results were the opposite: NBSS slopes of this study were more moderate than those by Sato et al. (2015). Thus, the differences in net mesh size are not considered to be a cause of the differences in NBSS slopes. These facts suggest that the differences in used instruments (OPC vs. ZooScan) would provide differences in NBSS.

As the differences between OPC and ZooScan, the former quantifies all the particles containing the samples, while the latter can identify zooplankton based on the obtained images. Thus, since ZooScan can distinguish zooplankton from non-living particles such as fecal pellet, fragment, and detritus, and not include those non-living particles for the analyses as was in this study (Vandromme et al., 2012). On the other hand, since OPC can not obtain imaging data, the separation between zooplankton and non-living particles is not possible, then NBSS derived from OPC includes all the particles, including the samples. Because the non-living particles (fecal pellet, fragment, detritus) are suffered from fragmentation, coprophagy, and coprorhexy by zooplankton and bacterial decomposition, their sizes are generally smaller than the zooplankton (Turner, 2002, 2015). Thus, when measuring the same zooplankton samples, data from OPC contains small-sized non-living particles, and their intercept and slope of NBSS would be higher and steeper, respectively, than those from ZooScan which calculated only on zooplankton data.

In a comparison of ZooScan with other instruments, there are several studies, including ZooScan with LOPC (Schultes and Lopes, 2009) and ZooScan with OPC (Naito et al., 2019) are available. Since LOPC and OPC included small-sized non-living particles, their NBSS slope tended to steep, while for ZooScan, the biovolumes of the large-sized gelatinous zooplankton (e.g. jellyfishes, doliolids, and salps) have been reported to quantify overestimation, thus their NBSS slope tends to moderate (Schultes and Lopes, 2009; Gorsky et al., 2010; Vandromme et al., 2012; Naito et al., 2019; Kwong and Pakhomov, 2021). While such characteristics or tendencies of instruments are available, when measuring the whole samples by using the same methods, since their characteristics or tendencies are common throughout the samples, the evaluation of their geographical, horizontal, or spatial changes is reported to be possible (Schultes and Lopes, 2009, 2012; Naito et al., 2019). Thus, in this study, we will make a comparison of the values of the NBSS slope or intercept obtained from this study only. For the other studies, we will make comparisons on the geographical patterns and not include NBSS values for the inter-study comparison.

 For the latitudinal changes of NBSS slope of zooplankton in the subarctic-subtropical North Pacific, there are several studies based on OPC analyses, and the NBSS slope has been reported to moderate for the subarctic region where dominated by the large-sized Neocalanus copepods (Fukuda et al., 2012; Shiota et al., 2013; Sato et al., 2015; Mishima et al., 2019). Within the region, seasonal changes in NBSS slope have also been reported, and moderate NBSS slopes in summer when development for the late copepodite stages have been observed for the large-sized *Neocalanus* copepods (Yamaguchi et al., 2014; Hikichi et al., 2018). Zooplankton biomass in the subarctic Pacific is predominated by the large-sized *Neocalanus* copepods (Ikeda et al., 2008). These facts suggest that moderate NBSS slopes are available for the region or season where and when dominated by the large-sized *Neocalanus* copepods.

For NBSS slope, significant relationships were observed with temperature, thus moderate slopes under low temperature, while steep slopes under high temperature (Fig. 13). For moderate NBSS slope of cold condition, it is due to the dominance of the large-sized copepods Neocalanus spp. especially in the epipelagic zones of the subarctic Pacific (Ikeda et al., 2008). Even for the subtropical region, the temperature of the deep-sea is low, and the deep-sea copepods inhabiting under such condition contains lipids in their body, having long longevity, and large-body sizes (Mauchline, 1998). Thus, under low-temperature conditions, NBSS may tend to have moderate slopes. On the other hand, under warm conditions, acceleration and high metabolism of zooplankton would be occurred, and no occurrence of large-sized copepods which having diapause phases (Mauchline, 1998). The steepest slopes of NBSS of this study were seen from the groups E and F which were observed for the epipelagic zones of the subtropical region (Table 5). These facts suggest that high temperatures under these conditions may prevent the occurrence of large-sized zooplankton there.

For the NBSS intercept, depth and salinity had significant relationships, and both showed a negative trend with the NBSS intercept (Fig. 13). Intercept of NBSS is reported to be a reflection of primary productivity at the given region and depth (Moore and Suthers, 2006; Zhou, 2006; Zhou et al., 2009; Gomez-Canchong et al., 2013). Since the primary productivity has been made at the sea surface where characterized by sufficient sunlight, the NBSS intercept would be high at the shallower depth. Since zooplankton biovolume decreased with increasing depth (Fig. 6), the NBSS intercept would be decreased with increasing depth. These depth trends of primary productivity and zooplankton biovolume induce negative relationships of NBSS intercept and depth mentioned above. For the interaction of NBSS intercept and salinity, the NBSS intercept was high (=high biovolume) under low salinity conditions, while the NBSS intercept was low (=low biovolume) under high salinity conditions (Fig. 13). In this study, the low salinity conditions were seen for the two stations in the subarctic Pacific and Okhotsk Sea (Fig. 3). The zooplankton biovolume of the epipelagic zones of these stations was high, especially at the near surface (Fig. 6b). These high zooplankton

 biovolumes there would induced high NBSS intercept under low salinity conditions. As depth trend for salinity, it increased with increasing depths throughout the stations (Fig. 3). The decreasing NBSS intercept with increasing salinity would be comparable that the NBSS intercept decreased with increasing depths, as mentioned before.

For size diversity, only depth had a strong significant effect, and the size diversity was low at the shallower depths and increased with increasing depths (Fig. 13). In terms of the zooplankton community, size diversity was high for groups A and D (Table 5) which observed for the deep layer of the subarctic region (Fig. 9). These facts suggest that size diversity would be high where the depths occurred zooplankton covering the broader size ranges from small to large.

In the present study, all parameters on zooplankton size spectra: intercept and slope of NBSS, and size diversity showed large geographical and vertical changes. Especially, the vertical discrepancy was detected at 150–500 m depths for all parameters, and these discrepancies were prominent in the transitional region and subtropical North Pacific, and East China Sea (Fig. 11). For these regions, depths of 150–500 m were serve as the boundaries to separate epipelagic zooplankton community and deep-sea zooplankton community, and below that layer, since zooplankton community was characterized with the that in the cold condition, intercept of NBSS would be lower, high size diversity due to dominance of the large-sized zooplankton (Fig. 13), then the moderate slope of NBSS may present (Fig. 11). While the narrower treated size ranges should be noted (Kwong and Pakhomov, 2021), NBSS and size diversity of this study clearly showed reflect of geographical and vertical changes in zooplankton community in the subarctic, transitional, and subtropical regions of the western North Pacific, and its three marginal seas: Okhotsk Sea, Japan Sea, and East China Sea.

### 5. Conclusions

Based on the vertically stratified net samples collected down to the deep layer (3000 m), regional and vertical changes in zooplankton abundance, biovolume, community structure, NBSS, and size diversity were evaluated at seven stations covering subarctic, transitional, and subtropical regions of western North Pacific and its marginal seas: Okhotsk Sea, Japan Sea, and East China Sea. Both abundance and biovolume decreased with increasing depths. Their depth-decreasing rates were more rapid for abundance than those in biovolume. The most governing environmental parameter on zooplankton abundance was depth, while the region was the most prominent for their biovolume. Based on the abundance data, zooplankton communities were clustered into eight groups. Each group was distributed for adjacent regions and depths, and the occurrence of the specialized community dominated by Phaeodaria and Ostracoda was seen for the deep layer of the Japan Sea. NBSS and size diversity showed clear vertical changes around 150–500 m depths. Above that layer, the intercept and slope of NBSS were high and steep, respectively, and it induced low size diversity there. On the other

hand, opposites: low NBSS intercept, moderate NBSS slope, and high size diversity were seen below that layer. This study showed regional and vertical changes in zooplankton abundance, biovolume, community structure, NBSS, size diversity, and its governing environmental parameters clearly.

# Acknowledgements

9

 The zooplankton samples used in this study were collected by T/S *Oshoro-Maru* of the Faculty of Fisheries, Hokkaido University. We express sincere thanks to the captain, crew, and scientists who onboard the cruise for their great help in collecting samples and obtaining hydrographic data used in this study. Part of this study was supported by Grant-in-Aid for Challenging Research (Pioneering) 20K20573, Scientific Research 22H00374 (A), 20H03054 (B), 19H03037 (B), and 17H01483 (A) from Japan Society for the Promotion of Science (JSPS). This study was partially supported by the Arctic Challenge for Sustainability II (ArCS II; JPMXD1420318865) and the Environmental Research and Technology Development Fund (JPMEERF20214002) of the Environmental Restoration and Conservation Agency of Japan.

#### References

- Arima, D., Yamaguchi, A., Nobetsu, T., Imai, I., 2016. Seasonal abundance, population structure, sex ratio and gonad maturation of *Metridia okhotensis* Brodsky, 1950 in the Okhotsk Sea: Analysis of samples collected by pumping up from deep water. Crustaceana 89 (2), 151–161. https://doi.org/10.1163/15685403-00003516
- Ducklow, H.W., Steinberg, D.K., Buesseler, K.O., 2001. Upper ocean carbon export and the biological pump. Oceanography 14: 50–58. <a href="https://doi.org/10.5670/oceanog.2001.06">https://doi.org/10.5670/oceanog.2001.06</a>
- Fukuda, J., Yamaguchi, A., Matsuno, K., Imai, I., 2012. Interannual and latitudinal changes in zooplankton abundance, biomass and size composition along a central North Pacific transect during summer: analyses with an Optical Plankton Counter. Plankton Benthos Res. 7 (2), 64–74. https://doi.org/10.3800/pbr.7.64
- Gomez–Canchong, P., Quinones, R.A., Brose, U., 2013. Robustness of size–structure across ecological networks in pelagic systems. Theor. Ecol. 6, 45–56. https://doi.org/10.1007/s12080-011-0156-7
- Gorsky, G., Ohman, M.D., Picheral, M., Gasparini, S., Stemmann, L., Romagnan, J.-B., Cawood, A., Pesant, S., García-Comas, C., Prejger, F., 2010. Digital zooplankton image analysis using the ZooScan integrated system. J. Plankton Res. 32 (3), 285–303. <a href="https://doi.org/10.1093/plankt/fbp124">https://doi.org/10.1093/plankt/fbp124</a>
- Herman, A.W., 1988. Simultaneous measurement of zooplankton and light attenuance with a new optical plankton counter. Cont. Shelf Res. 8 (2), 205–221. <a href="https://doi.org/10.1016/0278-278">https://doi.org/10.1016/0278-278</a>.

# 4343(88)90054-4

648

27 **2**664

29 3665

5679 56

5680

5681 $\overset{60}{6}82$ 

58

62

- Hikichi, H., Arima, D., Abe, Y., Matsuno, K., Hamaoka, S., Katakura, S., Kasai, H., Yamaguchi, A., 649 650 3 2018. Seasonal variability of zooplankton size spectra at Mombetsu Harbour in the **6**51 southern Okhotsk Sea during 2011: An analysis using an optical plankton counter. Reg. Stud. Mar. Sci. 20, 34–44. <a href="https://doi.org/10.1016/j.rsma.2018.03.011">https://doi.org/10.1016/j.rsma.2018.03.011</a>
  - Hirakawa, K., Imamura, A., 1993. Seasonal abundance and life history of Metridia pacifica (Copepoda: Calanoida) in Toyama Bay, southern Japan Sea. Bull. Plankton Soc. Japan 40 (1), 41–45. Available in: https://agriknowledge.affrc.go.jp/RN/2030511915.pdf
- 5 652 7 653 954 1655 12 1656 14 1657 16 1658 18 1659 2661 23 2662 25 2663 Honda, M.C., Wakita, M., Matsumoto, K., Fujiki, T., Siswanto, E., Sasaoka, K., Kawakami, H., Mino, Y., Sukigara, C., Kitamura, M., Sasai, Y., Smith, S.L., Hashioka, T., Yoshikawa, C., Kimoto, K., Watanabe, S., Kobari, T., Nagata, T., Hamasaki, K., Kaneko, R., Uchimiya, M., Fukuda, H., Abe, O., Saino, T., 2017. Comparison of carbon cycle between the western Pacific subarctic and subtropical time-series stations: highlights of the K2S1 project. J. Oceanogr. 73, 647–667. https://doi.org/10.1007/s10872-017-0423-3
  - Iguchi, N., Ikeda, T., Imamura, A., 1993. Growth and life cycle of a euphausiid crustacean (Euphausia pacifica Hansen) in Toyama Bay, southern Japan Sea. Bull. Japan Sea Natl. Fish. Res. Inst. 43, 69–81. https://agriknowledge.affrc.go.jp/RN/2010501890
    - Ikeda, T., 1990. Ecological and biological features of a mesopelagic ostracod, Conchoecia Biol. pseudodiscophora, in the Japan Sea. Mar. 107, 453-461. https://doi.org/10.1007/BF01313429
    - Ikeda, T., Imamura, A., 1992. Population structure and life cycle of the mesopelagic ostracod Conchoecia pseudodiscophora in Toyama Bay, southern Japan Sea. Mar. Biol. 113, 595– 601. https://doi.org/10.1007/BF00349703
    - Ikeda, T., Shiga, N., Yamaguchi, A., 2008. Structure, biomass distribution and trophodynamics of the pelagic ecosystem in the Oyashio region, western subarctic Pacific. J. Oceanogr. 64, 339-354. https://doi.org/10.1007/s10872-008-0027-z
    - Irisson, J.O., Ayata, S.D., Lindsay, D.J., Karp-Boss, L., Stemmann, L., 2022. Machine Learning for the study of plankton and marine snow from images. Ann. Rev. Mar. Sci. 14, 277–301. https://doi.org/10.1146/annurev-marine-041921-013023
    - Kitamura, M., Kobari, T., Honda, M.C., Matsumoto, K., Sasaoka, K., Nakamura, R., Tanabe, K., 2016. Seasonal changes in the mesozooplankton biomass and community structure in subarctic and subtropical time-series stations in the western North Pacific. J. Oceanogr. 72, 387–402. <a href="https://doi.org/10.1007/s10872-015-0347-8">https://doi.org/10.1007/s10872-015-0347-8</a>
    - Kobari, T., Moku, M., Takahashi, K., 2008. Seasonal appearance of expatriated boreal copepods in the Oyashio-Kuroshio mixed region. ICES J. Mar. Sci. 65 (3), 469-476.

27 **269**9

55/14 56

57715

57916  $^{60}_{671}7$ 

58

62

- Kwong, L.E., Pakhomov, E.A., 2021. Zooplankton size spectra and production assessed by two 684 685 3 different nets in the subarctic Northeast Pacific. J. Plankton Res. 43 (4), 527–545. 686 https://doi.org/10.1093/plankt/fbab039
- 5 687 Lalli, C.M., Parsons, T.R., 1997. Biological Oceanography: An Introduction, Second Edition. Butterworth-Heinemann, Burlington, MA, USA, p. 326. https://doi.org/10.1016/B978-0-7506-3384-0.X5056-7
- 7 688 9 1089 1690 12 1691 14 1692 16 1693 Makabe, R., Tanimura, A., Fukuchi, M., 2012. Comparison of mesh size effects on mesozooplankton collection efficiency in the Southern Ocean. J. Plankton Res. 34 (5), 432–436. https://doi.org/10.1093/plankt/fbs014
  - Mauchline, J., 1998. The biology of calanoid copepods. Adv. Mar. Biol., 33, 1–710. Available in: https://www.sciencedirect.com/bookseries/advances-in-marine-biology/vol/33/suppl/C
  - Miller, C.B., Wheeler, P.A., 2012. Biological Oceanography, Second Edition. John Wiley and Sons, Oxford, UK, p. 480. Available in: https://www.wiley.com/enus/Biological+Oceanography,+2nd+Edition-p-9781444333015
  - Mishima, K., Matsuno, K., Yamaguchi, A., 2019. Zooplankton size structure in the summer western North Pacific Ocean: Analysis by Optical Plankton Counter. Bull. Fac. Fish. Hokkaido Univ. 69 (1), 37–45. https://doi.org/10.14943/bull.fish.69.1.37
  - Moore, S.K., Suthers, I.M., 2006. Evaluation and correction of subresolved particles by the optical plankton counter in three Australian estuaries with pristine to highly modified catchments. J. Geophys. Res., 111, C05S04 https://doi.org/10.1029/2005JC002920
  - Morisita, M., 1996. On the influence of the sample size upon the values of species diversity. Japanese J. Ecol. 46 (3), 269–289. https://doi.org/10.18960/seitai.46.3 269
  - Naito, A., Abe, Y., Matsuno, K., Nishizawa, B., Kanna, N., Sugiyama, S., Yamaguchi, A., 2019. Surface zooplankton size and taxonomic composition in Bowdoin Fjord, north-western Greenland: A comparison of ZooScan, OPC and microscopic analyses. Polar Sci. 19, 120– 129. https://doi.org/10.1016/j.polar.2019.01.001
  - Nakamura, Y., Imai, I., Yamaguchi, A., Tuji, A., Suzuki, N., 2013. Aulographis japonica sp. nov. (Phaeodaria, Aulacanthida, Aulacanthidae), an abundant zooplankton in the deep sea of the Sea of Japan. Plankton Benthos Res. 8 (3), 107–115. https://doi.org/10.3800/pbr.8.107
  - Nishibe, Y., Ikeda, T., 2004. Vertical distribution, abundance and community structure of oncaeid copepods in the Oyashio region, western subarctic Pacific. Mar. Biol. 145, 931-941. https://doi.org/10.1007/s00227-004-1392-9
  - Nishibe, Y., Kobari, T., Ota, T., 2010. Feeding by the cyclopoid copepod Oithona similis on the microplankton assemblage in the Oyashio region during spring. Plankton Benthos Res., 5

718 (2), 74–78. https://doi.org/10.3800/pbr.5.74

5549 56

5750

58

62

- Nishibe, Y., Takahashi, K., Ichikawa, T., Hidaka, K., Kurogi, H., Sagawa, K., Saito, H., 2015. 719 7220 3 Degradation of discarded appendicularian houses by oncaeid copepods. Limnol. Oceanogr. 60 (3), 967–976. https://doi.org/10.1002/lno.10061
- Nunn, A.D., Tewson, L.H., Cowx, I.G., 2012. The foraging ecology of larval and juvenile fishes. Rev. Fish. Biol. Fisheries 22, 377–408. https://doi.org/10.1007/s11160-011-9240-8
  - Omori, M., Tanaka, O., 1967. Distribution of some cold-water species of copepods in the Pacific off east-central Honshu, J. 23 water Japan. Oceanogr. (2),63-73.https://doi.org/10.5928/kaiyou1942.23.63
  - Ozawa, M., Yamaguchi, A., Ikeda, T., Watanabe, Y., Ishizaka, J., 2007. Abundance and community structure of chaetognaths from the epipelagic through abyssopelagic zones in the western North Pacific and its adjacent seas. Plankton Benthos Res. 2 (4), 184–197. https://doi.org/10.3800/pbr.2.184
  - Padmavati, G., Ikeda, T., Yamaguchi, A., 2004. Life cycle, population structure and vertical distribution of *Metridia* spp. (Copepoda: Calanoida) in the Oyashio region (NW Pacific Ocean). Mar. Ecol. Prog. Ser. 270, 181–198. https://doi.org/10.3354/meps270181
  - Picheral, M., Colin, S., Irisson, J.-O., 2017. EcoTaxa, a tool for the taxonomic classification of images. https://ecotaxa.obs-vlfr.fr/ [accessed 2 May 2023].
  - Sato, K., Matsuno, K., Arima, D., Abe, Y., Yamaguchi, A., 2015. Spatial and temporal changes in zooplankton abundance, biovolume, and size spectra in the neighboring waters of Japan: analyses using optical plankton Zool. Stud. 54, 18 an counter. https://doi.org/10.1186/s40555-014-0098-z
  - Schultes, S., Lopes, R.M., 2009. Laser Optical Plankton Counter and Zooscan intercomparison in tropical and subtropical marine ecosystems. Limnol. Oceanogr. Methods 7 (11), 771–784. https://doi.org/10.4319/lom.2009.7.771
  - Shiota, T., Abe, Y., Saito, R., Matsuno, K., Yamaguchi, A., Imai, I., 2013. Spatial changes in mesozooplankton community structure in the North Pacific: Analyses by Optical Plankton Counter. Bull. Fac. Fish. Hokkaido Univ. 63 (3), 13–22. Available in: http://hdl.handle.net/2115/53985
  - Stamieszkin, K., Pershing, A.J., Record, N.R., Pilskaln, C.H., Dam, H.G., Feinberg, L.R., 2015. Size as the master trait in modeled copepod fecal pellet carbon flux. Limnol. Oceanogr. 60 (6), 2090–2107. https://doi.org/10.1002/lno.10156
  - Steinberg, D.K., Van Mooy, B.A.S., Buesseler, K.O., Boyd, P.W., Kobari, T., Karl, D.M., 2008a. Bacterial vs. zooplankton control of sinking particle flux in the ocean's twilight zone. Limnol. Oceanogr. 53 (4), 1327–1338. https://doi.org/10.4319/lo.2008.53.4.1327

- Steinberg, D.K., Cope, J.S., Wilson, S.E., Kobari, T., 2008b. A comparison of mesopelagic 753 754mesozooplankton community structure in the subtropical and subarctic North Pacific Ocean. Deep-Sea Res. II 55, 1615–1635. https://doi.org/10.1016/j.dsr2.2008.04.025
- 755 3 756 5 767 758 99 1760 12 1761 14 1762 16 1763 Sudo, H., 1986. A note on the Japan Sea proper water. Prog. Oceanogr. 17 (3-4), 313-376. https://doi.org/10.1016/0079-6611(86)90052-2
  - Suthers, I.M., Taggart, C.T., Rissik, D., Baird, M.E., 2006. Day and night ichthyoplankton assemblages and zooplankton biomass size spectrum in a deep ocean island wake. Mar. Ecol. Prog. Ser. 322, 225–238. https://doi.org/10.3354/meps322225
    - Takahashi, K., Kuwata, A., Sugisaki, H., Uchikawa, K., Saito, H., 2009. Downward carbon transport by diel vertical migration of the copepods Metridia pacifica and Metridia okhotensis in the Oyashio region of the western subarctic Pacific Ocean. Deep-Sea Res. 
      ☐ 56, 1777–1791. https://doi.org/10.1016/j.dsr.2009.05.006
    - Taki, K., 2006. Studies on fisheries and life history of Euphausia pacifica Hansen off northeastern Japan. Bull. Fish. Res. 18, 41–165. Available in: https://www.fra.affrc.go.jp/bulletin/bull/bull18/taki.pdf
    - Taki, K., 2011. Distribution and population structure of *Thysanoessa inspinata* and its dominance among euphausiids off northeastern Japan. J. Plankton Res. 33, 891–906. https://doi.org/10.1093/plankt/fbq162
    - Takizawa, T., 1982. Characteristics of the Soya warm current in the Okhotsk Sea. J. Oceanogr. Soc. Japan 38, 281–292. https://doi.org/10.1007/BF02114532
    - Terazaki, M., Tomatsu, C., 1997. A vertical multiple opening and closing plankton sampler. J. Adv. Mar. Sci. Tech. Soc. 3 (2),127–132. Available in: http://amstec.jp/book/journal\_data/vol3B01.pdf

57584 56

5785 58

**57**986  $^{60}_{6787}$ 

62

- Turner, J., 2002. Zooplankton fecal pellets, marine snow and sinking phytoplankton blooms. Aquat. Microb. Ecol. 27, 57–102. https://doi.org/10.3354/ame027057
- Turner, J., 2004. The importance of small planktonic copepods and their roles in pelagic marine food 255-266. webs. Zool. Stud. 43, Available in: https://zoolstud.sinica.edu.tw/Journals/43.2/255.pdf
- Turner, J., 2015. Zooplankton fecal pellets, marine snow, phytodetritus and the ocean's biological pump. Prog. Oceanogr. 130, 205–248. https://doi.org/10.1016/j.pocean.2014.08.005
- Vandromme, P., Stemmann, L., Garcia-Comas, C., Berline, L. Sun, X., Gorsky, G., 2012. Assessing biases in computing size spectra of automatically classified zooplankton from imaging systems: A case study with the ZooScan integrated system. Methods Oceanogr. 1–2, 3–21. https://doi.org/10.1016/j.mio.2012.06.001
- Vinogradov, M.E., 1968. Vertical Distribution of the Oceanic Zooplankton. Academy of Science of

the USSR, Institute of Oceanography (in Russian, English translation by Israel Program for Scientific Translations). Keter Press, Jerusalem, p. 339.

 $\frac{29}{305}$ 

58<u>1</u>9 

- Yamaguchi, A., 2015. Inter–oceanic comparison of planktonic copepod ecology (vertical distribution, abundance, community structure, population structure and body size) between the Okhotsk Sea and Oyashio region in autumn. J. Nat. Hist. 49 (45–48), 2743–2757. https://doi.org/10.1080/00222933.2015.1022616
- Yamaguchi, A., Watanabe, Y., Ishida, H., Harimoto, T., Furusawa, K., Suzuki, S., Ishizaka, J., Ikeda, T., Takahashi, M.M., 2002a. Community and trophic structures of pelagic copepods down to greater depths in the western subarctic Pacific. Deep-Sea Res. I 49 (6), 1007–1025. https://doi.org/10.1016/S0967-0637(02)00008-0
- Yamaguchi, A., Watanabe, Y., Ishida, H., Harimoto, T., Furusawa, K., Suzuki, S., Ishizaka, J., Ikeda, T., Takahashi, M.M., 2002b. Structure and size distribution of plankton communities down to the greater depths in the western North Pacific Ocean. Deep-Sea Res. II 49 (24–25), 5513–5529. <a href="https://doi.org/10.1016/S0967-0645(02)00205-9">https://doi.org/10.1016/S0967-0645(02)00205-9</a>
- Yamaguchi, A., Watanabe, Y., Ishida, H., Harimoto, T., Furusawa, K., Suzuki, S., Ishizaka, J., Ikeda, T., Takahashi, M.M., 2004. Latitudinal differences in the planktonic biomass and community structure down to the greater depths in the western north pacific. J. Oceanogr. 60 (4), 773–787. <a href="https://doi.org/10.1007/s10872-004-5770-1">https://doi.org/10.1007/s10872-004-5770-1</a>
- Yamaguchi, A., Watanabe, Y., Ishida, H., Harimoto, T., Furusawa, K., Maeda, M., Ishizaka, J., Ikeda, T., Takahashi, M.M., 2005. Biomass and chemical composition of net-plankton down to greater depths (0–5800 m) in the western North Pacific Ocean. Deep-Sea Res. I 52 (2), 341–353. <a href="https://doi.org/10.1016/j.dsr.2004.09.007">https://doi.org/10.1016/j.dsr.2004.09.007</a>
- Yamaguchi, A., Matsuno, K., Abe, Y., Arima, D., Ohgi, K., 2014. Seasonal changes in zooplankton abundance, biomass, size structure and dominant copepods in the Oyashio region analysed by an optical plankton counter. Deep-Sea Res. I 91, 115–124. <a href="https://doi.org/10.1016/j.dsr.2014.06.003">https://doi.org/10.1016/j.dsr.2014.06.003</a>
- Yamaguchi, A., Matsuno, K., Homma, T., 2015. Spatial changes in the vertical distribution of calanoid copepods down to great depths in the North Pacific. Zool. Stud. 54, 13. https://doi.org/10.1186/s40555-014-0091-6
- Yokoi, Y., Yamaguchi, A., Ikeda, T., 2008. Regional and inter-annual changes in the abundance, biomass and community structure of mesozooplankton in the western North Pacific in early summer; an analyzed with an optical plankton counter. Bull. Plankton Soc. Japan 55 (1), 9–24. Available in: <a href="https://agriknowledge.affrc.go.jp/RN/2010786004">https://agriknowledge.affrc.go.jp/RN/2010786004</a>
- Zenkevitch, L., 1963. Biology of the Seas of the U.S.S.R. Institute of Oceanography (in Russian, English translation by S. Botcharkaya). George Allen and Unwin Ltd., London, p. 955.

 Zhou, M., 2006. What determines the slope of a plankton biomass spectrum? J. Plankton Res. 28 (5), 437–448. <a href="https://doi.org/10.1093/plankt/fbi119">https://doi.org/10.1093/plankt/fbi119</a>

Zhou, M., Tande, K.S., Zhu, Y., Basedow, S., 2009. Productivity, trophic levels and size spectra of zooplankton in northern Norwegian shelf regions. Deep-Sea Res. II 56 (21–22), 1934–1944. <a href="https://doi.org/10.1016/j.dsr2.2008.11.018">https://doi.org/10.1016/j.dsr2.2008.11.018</a>

### Table and Figure legends

- Table 1. Sampling data on vertical stratified samplings by VMPS equipped 63 µm mesh at the seven stations located various regions of the neighboring waters of Japan. Note that the depth strata was varied with the region.
- Table 2. Regression statistics of abundance (Abu: ind. m<sup>-3</sup>) and biovolume (Bio: mm<sup>3</sup> m<sup>-3</sup>) along with depth (D: m) for the seven stations neighboring waters of Japan. As regressions, power models were used:  $\log_{10}Abu = a \log_{10}D + b$  or  $\log_{10}Bio = a \log_{10}D + b$ , where a and b were fitted constants. For details of data, see Fig. 6. \*: p < 0.05, \*\*: p < 0.01, \*\*\*: p < 0.001, ns: not significant.
- Table 3. Results of ANCOVA on zooplankton abundance and biovolume, with the sampling depth (m) and region (station) (cf. Table 1) applied as independent variables. *df*: degree of freedom, *SS*: sum of squares.
- Table 4. Mean abundance (ind.  $m^{-3}$ ) of each zooplankton taxon at eight clustered groups (A-H) identified by Bray-Curtis similarity analysis (cf. Fig. 7). The numbers in the parentheses indicate the number of samples included in each group. Differences between groups were tested by one-way ANOVA and post hoc Tukey-Kramer test. For the results of the Tukey-Kramer test, any groups not connected by the underlines are significantly different (p<0.05). -: no occurrence, \*: p<0.05, \*\*: p<0.01, \*\*\*: p<0.001, NS: not significant. For abundance, the upper three most dominant taxa/species are shown by the bold and underlines.
- Table 5. Inter-group differences in zooplankton size relataed variables (slopes and intercepts of NBSS and size diversities) evaluated for zooplankton samples collected from 0–3000 m depths of the seven sampling stations at neighboring waters of Japan. For details of the location of the stations and distribution of each zooplankton community clustered by the zooplankton abundance data, see Figs. 1 and 9, respectively. For detailed data of NBSS and size diversity see Figs. 10 and 11, respectively.
- Fig. 1. Location of the seven sampling stations neighboring waters of Japan. OK: Okhotsk Sea, JS1: Japan Sea station 1, JS2: Japan Sea station 2, ECS: East China Sea, SA: subarctic Pacific, TR: transitional Pacific, ST: subtropical Pacific. Approximate flow directions of the major currents are shown with the arrows in the panel.
- Fig. 2. Vertical changes in temperature, salinity and dissolved oxygen at the seven stations neighboring waters of Japan. OK: Okhotsk Sea, JS1: Japan Sea station 1, JS2: Japan Sea station 2, ECS: East China Sea, SA: subarctic Pacific, TR: transitional Pacific, ST: subtropical Pacific. Symbols denote mean values for the sampling depths of VMPS at each station.
- Fig. 3. T-S diagram at the seven stations neighboring waters of Japan. OK: Okhotsk Sea, JS1: Japan

- 863 Sea station 1, JS2: Japan Sea station 2, ECS: East China Sea, SA: subarctic Pacific, TR: transitional Pacific, ST: subtropical Pacific. Symbols denote mean values for the sampling 864  $\frac{865}{3}$ depths of VMPS at each station.
- 866 Fig. 4. Vertical changes in zooplankton abundance and their taxonomic composition at the seven 5 867 stations neighboring waters of Japan. Note that abundance scales are in log-scales. OK: Okhotsk Sea, JS1: Japan Sea station 1, JS2: Japan Sea station 2, ECS: East China Sea, SA: subarctic Pacific, TR: transitional Pacific, ST: subtropical Pacific.
  - Fig. 5. Vertical changes in zooplankton biovolume and their taxonomic composition at the seven stations neighboring waters of Japan. Note that biovolume scales are in log-scales. OK: Okhotsk Sea, JS1: Japan Sea station 1, JS2: Japan Sea station 2, ECS: East China Sea, SA: subarctic Pacific, TR: transitional Pacific, ST: subtropical Pacific.
  - Fig. 6. Vertical changes in zooplankton abundance (a) and biovolume (b) at the seven stations neighboring waters of Japan. OK: Okhotsk Sea, JS1: Japan Sea station 1, JS2: Japan Sea station 2, ECS: East China Sea, SA: subarctic Pacific, TR: transitional Pacific, ST: subtropical Pacific.
  - Fig. 7. Result of cluster analysis based on the mesozooplankton abundance of each sample collected from 0–3000 m strata of the seven stations neighboring waters of Japan. OK: Okhotsk Sea, JS1: Japan Sea station 1, JS2: Japan Sea station 2, ECS: East China Sea, SA: subarctic Pacific, TR: transitional Pacific, ST: subtropical Pacific. For samples, numbers after underbar represent depth layers (m).
  - Fig. 8. Two-dimensional map by non-metric multidimensional scaling method (NMDS) of zooplankton communities specified by the depth-station complex data. Eight groups (group A-H) that clustered according to the Bray-Curtis similarity index (Fig. 7) are shown by the different symbols. Arrows indicate directions of significant environmental parameters. Lat.: latitude, Dep.: depth, Temp.: temperature, Sal.: salinity, DO: dissolved oxygen.
  - Fig. 9. Spatial and vertical distribution of zooplankton community groups identified by Bray-Curtis similarity index (cf. Fig. 7). Sampling depth at each station is shown by the symbols. Note that depth scale is in log-scale. OK: Okhotsk Sea, JS1: Japan Sea station 1, JS2: Japan Sea station 2, ECS: East China Sea, SA: subarctic Pacific, TR: transitional Pacific, ST: subtropical Pacific.

5894 56

589558

5896 $\overset{60}{897}$ 

62

63 64 65

Fig. 10. Vertical changes in normalized biovolume size spectra (NBSS) at various depth strata of the seven sampling stations neighboring waters of Japan. Note that NBSS regressions are highly significant ( $r^2$ =0.15-0.9, p<0.05) for all sampling depths. OK: Okhotsk Sea, JS1: Japan Sea station 1, JS2: Japan Sea station 2, ECS: East China Sea, SA: subarctic Pacific, TR: transitional Pacific, ST: subtropical Pacific.

- Fig. 11. Vertical changes in slope and intercept of the normalized biovolume size spectra (NBSS) and size diversity at various depth strata of the seven sampling stations neighboring waters of Japan. OK: Okhotsk Sea, JS1: Japan Sea station 1, JS2: Japan Sea station 2, ECS: East China Sea, SA: subarctic Pacific, TR: transitional Pacific, ST: subtropical Pacific.
- Fig. 12. Scatter plots between slope and intercept of NBSS (a), size diversity and slope of NBSS (b), and size diversity and intercept of NBSS (c) at seven stations neighboring waters of Japan. OK: Okhotsk Sea, JS1: Japan Sea station 1, JS2: Japan Sea station 2, ECS: East China Sea, SA: subarctic Pacific, TR: transitional Pacific, ST: subtropical Pacific. Differences in colors represent sampling depths (0–200, 200–1000, and 1000–3000 m).
- Fig. 13. Result of GAMs based on anomalies of the slope and intercept of NBSS and size diversity with environmental parametrs (depth, temperature and salinity). \*\*: p<0.01, \*\*\*: p<0.001.

Declaration of Interest Statement
-----------------------------------

Yamamae et al.

The authors declare that they have no conflict of interest.

Electronic Supplement 1

Click here to access/download

e-Component

Electronic Supplement 1.xlsx